Iron Oxide Based MR Contrast Agents: from Chemistry to Cell Labeling

S. Laurent*, S. Boutry, I. Mahieu, L. Vander Elst and R.N. Muller

Department of General, Organic and Biomedical Chemistry, NMR and Molecular Imaging Laboratory, University of Mons, Avenue Maistriau, 19, 7000 Mons, Belgium

Abstract: Superparamagnetic iron oxide nanoparticles can be used for numerous applications such as MRI contrast enhancement, hyperthermia, detoxification of biological fluids, drug delivery, or cell separation. In this work, we will summarize the chemical routes for synthesis of iron oxide nanoparticles, the fluid stabilization, and the surface modification of superparamagnetic iron oxide nanoparticles. Some examples of the numerous applications of these particles in the biomedical field mainly as MRI negative contrast agents for tissue-specific imaging, cellular labeling, and molecular imaging will be given.

Larger particles or particles displaying a non-neutral surface (thanks to their coating or to a cell transfection agent with which they are mixed) are very useful tools, although the cells to be labeled have no professional phagocytic function. Labeled cells can then be transplanted and monitored by MRI in a broad spectrum of applications.

Direct *in vivo* magnetic labeling of cells is mainly performed by intravenous injection of long-circulating iron oxide-based MRI contrast agents, which can extravasate and/or undergo a cellular uptake in an amount sufficient to allow an MRI visualization of areas of interest such as inflamed regions or tumors.

Particles with long circulation times, or able to induce a strong negative effect individually have been also modified by conjugation to a ligand, so that their cellular uptake, or at least their binding to the cell surface, could occur through a specific ligand-receptor interaction, *in vivo* as well as *in vitro*. Thus, experimentally as well as in a few trials on humans, iron oxide particles currently find promising applications.

Keywords: iron oxide nanoparticles, MRI, contrast agents, cell labeling, superparamagnetic nanoparticles, cellular uptake.

1. INTRODUCTION

The synthesis of superparamagnetic iron oxide nanoparticles has been intensively developed for many applications like: targeted drug and gene delivery [1, 2], contrast agents for use in magnetic resonance imaging (MRI), hyperthermia, detoxification of biological fluids, drug delivery, or cell separation [3-11]. All these biomedical applications require that the nanoparticles have high magnetization values, a size smaller than 100 nm, and a narrow particle size distribution. A number of approaches have been described to produce magnetic nanoparticles, including mechanical attrition (grinding fracture of large materials to form nanosize compounds), physical vapor deposition (assemblage of individual atoms to form nanosystems), and solution chemistry [12-15]. This last kind of technique gives the best results with control of the particle's size and size distribution. In this work, we will summarize the chemical routes for synthesis of iron oxide nanoparticles, the fluid stabilization, and the surface modification of these superparamagnetic nanoparticles. Some examples of the numerous applications of these particles, mainly as negative contrast agents, in biomedical research fields such as tissue-specific MRI, cellular MRI, and molecular MRI, will be given [5, 16-18].

2. SYNTHESIS OF MAGNETIC NANOPARTICLES

2.1. Classic Synthesis by Precipitation

Magnetite is synthesized by two fundamental processes: size reduction [19] and aqueous precipitation. The major advantage of precipitation reactions is that large amounts of nanoparticles can be obtained, however it is difficult to control the size because only kinetic factors are available to control growth. The first controlled preparation of superparamagnetic iron oxide particles using alkaline precipitation of $FeCl_3$ and $FeCl_2$ was performed by Massart [20] (eq. 1). These particles have a large size distribution, but size selection titration can reduce the heterodispersity [21].

$$2\ Fe^{3+} + Fe^{2+} + 8\ OH^- \longrightarrow FeO.Fe_2O_3 + 4\ H_2O \qquad (1)$$

Magnetite nanoparticles, prepared by coprecipitation of Fe^{2+} and Fe^{3+} with NH_4OH, can be stabilized with silica to form well dispersed magnetic silica nanospheres. The size of the particles can be controlled by changing the ratio of SiO_2 to Fe_3O_4. Aminosilane has been covalently coupled to the surface of the magnetic silica nanoparticles [22-24] and activated by glutaraldehyde to graft BSA [25].

2.2. High Temperature Reactions

Hydrothermal reactions are aqueous reactions carried out in high pressure reactors or autoclaves where the pressure can be over 2000 psi and the temperature above 200°C. Hydrophobic magnetite particles with a narrow size distribution have been prepared by thermal decomposition of $Fe(CO)_5$ in octyl ether solution of oleic acid and by consecutive aeration. These nanoparticles were then converted into magnetite core/silica shell with hydrophilic and processible aminopropyl groups on their surfaces [26].

Others used a surfactant, sodium bis(2-ethylhexyl)sulfosuccinate (AOT), to prepare ferromagnetic Fe_3O_4 nanoparticles with a diameter of ~27 nm by a hydrothermal route [27].

Sun *et al.* have described a high temperature reaction of iron (III) acetylacetonate with 1,2-hexadecanediol in pres-

*Address correspondence to this author at the Department of General, Organic and Biomedical Chemistry, NMR and Molecular Imaging Laboratory, University of Mons, Avenue Maistriau, 19, 7000 Mons, Belgium; Tel: 00.32.65373525; Fax: 00.32.65673520;
E-mail: sophie.laurent@umons.ac.be

0929-8673/09 $55.00+.00

ence of oleic acid and oleylamine to obtain monodisperse magnetite nanoparticles. The diameter of their hydrophobic particles can be tuned from 4 to 20 nm and can be transformed into hydrophilic ones by adding bipolar surfactant [28].

Park *et al*. have reported on a large scale synthesis of monodisperse crystals using inexpensive and non-toxic metal salts as reactants, in a single reaction without a size sorting process. The particle's size is controlled by varying the experimental conditions (reaction time, temperature, etc.) [29].

2.3. Reactions in Steric Environments

The aqueous precipitation of hydrated iron ions in bulk solutions creates sphere-like nanoparticles of various sizes. Several attempts have been reported to form well-defined iron oxide nanoparticles of controlled size using synthetic and biological nanoreactors. The constrained environments include: amphoteric surfactants to create water swollen reversed micellar structures in non-polar solvents [30-33], apoferritin protein cages [34, 35], and phospholipid membranes that form vesicles with iron oxide nanoparticles serving as solid supports [36, 37].

Surfactant molecules may spontaneously form aggregates with different sizes, micelles (1 to 10 nm), or microemulsions (10 to 100 nm) [38]. In the case of reverse micelles, water can be solubilized "inside" and the system can impose kinetic and thermodynamic constraints on particle formation like a nanoreactor. Water-in-oil microemulsions are created using amphoteric surfactants. In non-polar hydrocarbon solvents, the polar head group self-associates and forms micellar structures. The non-polar tails extend out into the solvent creating a thermodynamically stable dispersion. With the appropriate surfactant chemical composition and concentration, these micellar cores serve as constrained nanoreactor environments for the coprecipitation of aqueous iron salts [39].

The literature reports the use of sodium bis(2-ethylhexyl-sulfosuccinate) (AOT) [30, 31, 33] or cetyltrimethyl-ammonium bromide (CTAB) [22] as ionic surfactants. A reverse micelle nanoreactor approach using non-ionic surfactants avoids the complication of the presence of a complexing-functional species and offers great future potential.

Iron oxide can be prepared by the decomposition (by thermolysis or sonolysis) of organometallic precursors. Polymers, organic capping agents, or structural hosts are used to limit the size of the nanoparticle growth [40-51]. For example, iron oleate can be formed from decomposition of iron carbonyl in the presence of octyl ether and oleic acid at 100°C. After cooling to room temperature, $(CH_3)_3NO$ is added and the solution refluxed [52].

Nanostructured particles were also produced by sonochemical treatment of volatile organometallic precursors [53-59]. Addition of stabilizers or polymers during or post-sonication produces metal colloids. Shafi *et al.* have used sonochemical ways to prepare nanoparticles of Fe, Fe_3O_4, and Fe_2O_3 [55]. Oxide formation was also observed when the sonication was performed in aqueous solution and with non-carbonyl precursors [58, 59].

2.4. Sol-Gel Reactions

Sol-gel processing can be used to prepare iron oxide [60, 61]. The principal parameters that influence the kinetics and the growth reactions are: solvent, temperature, precursors, pH and agitation [62]. This method presents some advantages, like (i) the possibility to obtain materials with predetermined structure following experimental conditions, (ii) the achievement of pure amorphous phases, a monodispersity, and a good control of particle size, (iii) the control of the microstructure and the homogeneity of the reaction products, and (iv) the possibility to embed molecules which maintain their stability and properties within the sol-gel matrix.

Raileanu *et al.* [63] have prepared sol-gel nanocomposite materials (Fe_xO_y-SiO_2) by using alkoxide and aqueous routes. Different precursors of silica (tetramethoxysilane, methyltriethoxysilane, colloidal silica solution, etc.) were used to compare the structure and the properties of obtained nanoparticles. The structural and morphological results obtained by XRD, IR spectroscopy, TEM were correlated with the temperature dependence of the magnetic interactions investigated by Mossbauer spectroscopy.

2.5. Polyol Methods

The polyol process is a versatile chemical approach, which refers to the use of polyols (like diethylene glycol, for example) to reduce metal salts to metal particles. The method is a suitable way for preparing particles of a well controlled size [64]. The polyols often serve as high boiling solvents and reducing agents, as well as stabilizers to control the particle's growth and to prevent interparticle aggregation. Recently, Cai and Wan have developed an easy method to directly produce non-aggregated magnetite nanoparticles in liquid polyols [65].

2.6. Electrochemical Methods

Based on an electrochemical method previously described [66], Pascal *et al.* [67] have prepared 3-8 nm maghemite from an iron electrode immersed in an aqueous DMF solution in the presence of cationic surfactants. Adjustment of the current density allowed controlling the particle size. Electrochemical deposition under oxidizing conditions has also been used to prepare maghemite (Fe_2O_3) or magnetite (Fe_3O_4) [68].

2.7. Pyrolysis

Laser pyrolysis as a tool for the gas-phase synthesis of nanoparticles was recently illustrated by the preparation of iron-based nanostructures, where sensitized iron pentacarbonyl-based mixtures and ethylene as energy transfer agent were employed [69].

The product characteristics is related to the principal process conditions. Iron–carbon core-shell nanoparticles with a low mean size (about 4–5 nm) and modified morphologies were obtained by an increase of ethylene flow. In the case of γ-iron oxide nanopowder synthesis, low carbon contamination by ethylene depletion at increased system pressure was observed.

2.8. Sonolysis

The sonolysis of an aqueous solution of $Fe(CO)_5$ in the presence of sodium dodecyl sulfate has led to the formation of a stable hydrosol of amorphous Fe_3O_4 nanoparticles [70]. The amorphicity of iron oxide nanoparticles has been determined by X-ray diffraction and differential scanning calorimetry.

Superparamagnetic iron oxide nanoparticles (SPIO) with high magnetization and crystallinity have been synthesized by using a sonochemical method [71]. Ferrofluids from these nanoparticles coated with oleic acid as a surfactant were prepared. The coated SPIO could be easily dispersed in chitosan. They had a good stability and their hydrodynamic diameter was estimated to be 65 nm.

3. STABILIZATION OF MAGNETIC PARTICLES

The stabilization of the iron oxide particles is crucial for obtaining magnetic colloidal ferrofluids stable against aggregation in a magnetic field. The chemical surface properties of magnetic nanoparticles are very important for stability and vectorization. The surface iron act as Lewis acids and coordinate with molecules that donate lone pair electrons. So, in aqueous solution, the Fe atoms coordinate with water, which dissociates readily to leave the iron oxide surface hydroxyl functionalized. These hydroxyl groups are amphoteric and may react with acids or bases [72]. The isoelectric point is pH 6.8. Stabilization of magnetic particles can be achieved by electrostatic layer, steric repulsion, or by modifying the isoelectric point with a citrate or silica coating [73] (Fig. (**1**)).

Several approaches have been developed to coat iron oxide nanoparticles, including *in situ* coatings and post synthesis coatings. In the first approach, nanoparticles are coated during the synthesis; for example, Josephson *et al*. have developed a coprecipitation process in the presence of dextran [74].

The post-synthesis coating methods can use a variety of materials (polymers, phospholipids, silica derivatives, etc.).

3.1. Monomeric Stabilizers

Ionic surfactants prevent agglomeration due to attractive forces by creating repulsive forces originating from the proximity of like charged particles approaching one other. Functional groups like phosphates, sulfates, and carboxylates [75] are known to bind to the surface of magnetite.

The electrostatic repulsion is based on a charge balance of the surface atoms of the iron oxide and an ionic stabilizer. The surface electric charge attracts ions of opposite charge and creates an electric double layer. At pH values above the isoelectric point, the surface is negatively charged and ions of tetramethylammonium hydroxyde (TMAOH) stabilize magnetite. When the solution is at a pH below the isoelectric point, the particles can be stabilized with anions such as the ClO_4^- ion of perchloric acid. Lauric acid has been used to stabilize magnetite in chloroform. Gluconic acid may allow biological molecules to couple to iron oxide nanoparticles [76].

The carboxylates have important effects on the growth of iron oxide nanoparticles and their magnetic properties. Bee *et al*. have investigated the effect of the concentration of citrate ions on the size of maghemite particles [77]. Krishnamurti and Huang have studied the influence of citrate on the kinetics of Fe^{2+} oxidation and the resulting hydrolytic products of Fe^{3+} [78]. Huang and Wang have shown that the rate constant governing the oxidation of Fe^{2+} in the presence of inorganic ligands decreases as perchlorate, fluoride, nitrate, chloride, carbonate, sulfate, silicate and phosphate concentrations increase [79].

Liu and Huang showed that the presence of citric acid during iron oxide synthesis [80] caused significant decreases in the crystallinity of the iron oxides formed. Moreover, the presence of the citrate led to changes in the surface geome-

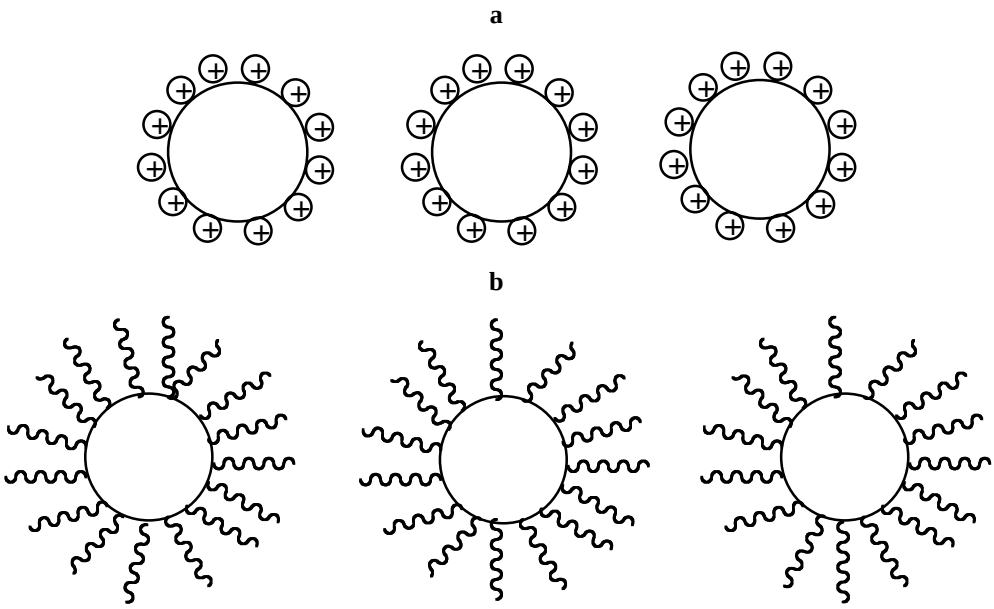

Fig. (1). Particles stabilized by (**a**) electrostatic layer and (**b**) steric repulsion.

try. Other studies on the influence of the carboxylate ions show similar results [81-83].

The steric stabilization of the magnetite surface can be tailored for dispersibility into aqueous media using amphiphilic surfactants. Phosphate containing surfactants for non-polar ferrofluid dispersions include: alkyl phosphonates/phosphates such as dodecylphosphonic acid (DDP), hexadecylphosphonic acid (HDP), and dihexadecyl phosphate (DHDP) [84]. Oleic acid is used as a steric stabilizer for iron oxide particle dispersions in hydrocarbon solvents [85-87]. One method is to form iron oxides by aqueous coprecipitation of the iron salts in the presence of oleic acid (C18) dissolved in a non-polar solvent. The adsorption occurs *via* interface mechanisms and extracts the particles into the non-polar carrier fluid. The transfer of iron oxide into the oil phase is achieved by modifying the high-energy hydrophilic surface to a lower energy hydrophobic surface. However, oleic acid cannot form stable dispersions in water. Khalafalla *et al.* reported that fatty acids with C10 to C15 are capable of making stable water-based dispersions [88].

Shimoiizaka *et al.* first described the use of fatty acids to create iron oxide nanoparticles dispersible in water *via* the formation of a bilayer surfactant system [89]. The process involves the formation of magnetite in the presence of a fatty acid such as oleic acid, which extracts magnetite into a non-polar carrier fluid. Then, the carrier fluid is removed and another amphiphilic surfactant (a fatty acid) is added and the mixture is redispersed in water [90]. The combination of surfactants varies: oleic acid with polyethyleneoxyphenyl ether or sodium dodecylbenzyl sulphonate [91], mixture of unsaturated and saturated fatty acids or saturated fatty acids for both layers [92].

3.2. Silica Coating of Iron Oxide Nanoparticles

A silica layer on the surface of iron oxide nanoparticles may be useful to: (i) create a functional surface to tailor dispersibility of the nanoparticles, (ii) form a layer to control electron tunneling between particles, which may be important in charge transport or magnetooptics, and (iii) provide better protection against toxicity.

Silica colloids embedded with superparamagnetic iron oxide nanoparticles have been synthesized by combining commercial ferrofluids with the Stöber process [93]. Organophilic iron oxide nanoparticles were extracted from a ferrofluid and redispersed in toluene. The suspension was then added to an alcoholic medium to produce emulsion drops consisting of aggregates of iron oxide nanoparticles and toluene. Tetraethylorthosilicate introduced into the system formed silica coating around each emulsion drop. The final size of silica colloids depended on the concentration of iron oxide nanoparticles and the type of solvent used for the Stöber synthesis. Larger colloids were obtained at lower concentrations of iron oxide nanoparticles and in alcohols with higher molecular weights.

3.3. Polymeric Stabilizers

Groman *et al.* suggested the use of dextran (Mw= 10000-15000 g/mol) as a surfactant during the formation of iron oxide particles [94]. Pardoe *et al.* offered detailed magnetic and structural properties of iron oxide formed in the presence of dextran (40000 g/mol) [95]. Molday and Mackenzie also reported the formation of magnetite in the presence of dextran 40000 [96]. The dextran was functionalized after iron oxide stabilization by oxidation with periodate and reaction of the amino groups of proteins.

Iron oxide particles formed in the presence of aqueous polyvinyl alcohol (PVA, 30-40 kg/mol) have been found to create necklace-like chains of ~ 100 nm with Fe content of 7.7 wt % [97]. In this study, superparamagnetic nanosized magnetite particles were prepared by controlled coprecipitation of Fe^{2+} and Fe^{3+} in the presence of highly hydrophilic poly(vinylalcohol phosphate)(PVAP) and the impact of polymer concentration on particle size, size distribution, colloidal stability, and magnetic property was studied. The aqueous suspension of magnetite, prepared using 1% PVAP solution, was found to be stable for four weeks at pH 5-8. X-ray diffractograms showed the formation of nanocrystalline inverse spinel phase magnetite. Transmission Electron Microscopy showed that cubic magnetite particles of about 5.8 nm size were well dispersed. Dynamic Light Scattering measurement showed a narrow distribution of the hydrodynamic size of particle aggregates. Infrared spectra of samples showed a strong Fe--O--P bond on the oxide surface. UV-visible studies showed that the aqueous dispersion of magnetite formed by using 1% PVAP solution was stable at least for four weeks without any deterioration of particle size. Magnetization measurements at room temperature confirmed the superparamagnetic nature of polymer coated magnetite nanoparticles [97].

Other polymers have been used, like polymethacrylic acid [98], poly(ethyleneoxide)-b-poly(methacrylic acid) [99], and poly(ethylene oxide) [100]. One example is the preparation of iron oxide nanoparticles stabilized with Brij® (polyoxyethylene (10) oleyl ether, $C_{18}H_{35}(OCH_2CH_2)_nOH$) for MR contrast agents [101]. Magnetite particles have been synthesized also in the presence of 50 wt% dicarboxypolyethylene glycol (DCPEG, ~2000 g/mol) in water and then the DCPEG coated magnetite bound to lipase using a water soluble carbodiimide [102].

Another approach is to use surface initiated polymerization to grow polymer chains on the surface of iron oxide particles. ATRP (atom transfer radical polymerization) has become a method of choice for this procedure: free radical initiators are first immobilized onto the surfaces of iron oxide core followed by polymer growth outwards to a radius structure [103]. ATRP offers several advantages over other polymerization methods, such as control of molecular weight and molecular weight distribution [104].

4. METHODS FOR VECTORIZATION OF THE PARTICLES

For biological applications, like molecular imaging, nanoparticles must be highly stable in aqueous ionic solutions at physiological pH and vectorized. Several covalent conjugation strategies using amine, carboxyl, aldehyde, or thiol groups exposed on the surface of nanoparticles have been developed [105].

Vectors grafted on the particles' surface must be able to recognize the target cells or tissues. Particles must be non-

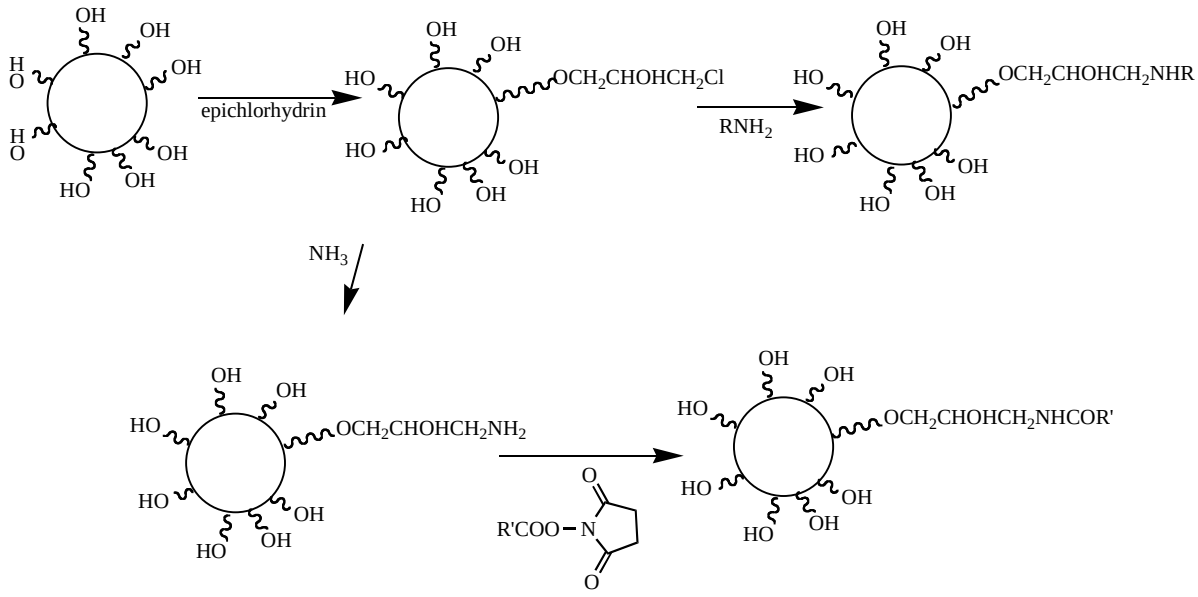

Fig. (2). Synthesis of grafted particles *via* epichlorhydrin.

toxic and should remain in the circulation for a time long enough to reach their target.

An oxidative conjugation strategy has been used in previous studies: it produces aldehydes on the dextran coating of the iron oxides [106], but a substantial loss of the biological activity of the protein has been observed. To minimize this effect, Hogemann *et al*. have linked the protein and the iron oxide particle *via* a linker molecule. Their results suggest that the oxidative conjugation chemistry significantly interferes with the binding of the conjugates of the receptor. Current efforts are devoted in the direction of non-oxidative strategies. The target molecules are covalently linked through a 2 or 3 step-reaction sequence (Fig. (**2**)): epichlorhydrin is first coupled to the hydroxyl groups of the dextran coating of the Fe_3O_4 crystals to give a terminal halogen derivative that can be used to link any molecule containing an amine function (peptide, protein, antibodies or ammonia). The first step, consisting in the reaction of dextran with epichlorhydrin, has been described by Josephson *et al*. [107]. Folate, for instance, can be attached to the surface of an aminated nanoparticle through the reaction between activated NHS-folate ester and the amino groups.

The grafting of vector molecules on the particles can also be achieved with 2,3-dimercaptosuccinic acid (DMSA) and N-succinimidyl 3-(2-pyridyldithio)propionate (SPDP) [108, 109]. In this case, the nanoparticular system is constituted by two subunits: the particle coated with the chelating agent DMSA and the ligand linked to SPDP through a peptide bond. These subunits are joined by an S-S bridge between DMSA and SPDP (Fig. (**3**)).

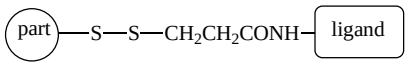

Fig. (3). Particles with S-S bridge.

Recently, magnetite nanoparticles coated with an aminosilane coupling agent, SG-Si900 were covalently linked using glutaraldehyde as cross-linker [110]. Alternatively, vectors with carboxylic functions can be directly grafted on the silica coated particles using EDC to activate the carboxyl groups.

The silane coupling materials (like 3-aminopropyltrimethoxysilane or p-aminophenyl trimethoxysilane) [111] are able to adsorptively or covalently bind to the metal oxide and to form covalent bonds with biomolecules. The mechanism of the silane coupling agents' reaction according to Arkles [112] is given in Fig. (**4**).

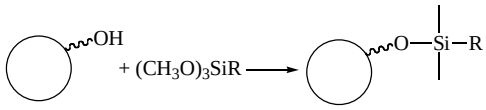

Fig. (4). Chemical reaction of silane coupling agents on magnetic particles.

Surface chemistry involving reactions with alkyltrialkoxysilane or trichloroalkylsilane compounds [113, 114] or with functional groups have been prepared by reaction with alkylsilane derivatives containing different functional groups ($SiR_3(CH_2)_nX$: R=Cl, OCH_3, OC_2H_5, etc.; n=3-17; X=CH_3, CN, CO_2CH_3, etc.) to form ether bonds. Particles with ω-hydroxyl or primary amine groups have been prepared by reaction of the surface with alkylalkoxysilane compounds ($Si(OEt)_3(CH_2)_3CO_2CH_3$, $Si(OEt)_3(CH_2)_3NH_2$, etc.) or with trichloroalkylsilane derivatives ($SiCl_3(CH_2)_3CO_2CH_3$, $SiCl_3(CH_2)_3CN$, etc.) followed by diborane reduction. Particles with thiol functions have been formed by thiourea reaction and hydrolysis of the ω-phenylchloromethyl.

Recently, Sun *et al*. have developed the "click chemistry" (azide-alkyne reaction) for vectorization of iron oxide nanoparticles with small molecules [115]. These authors show an easy preparation of stable particles bearing azido or alkine groups able of reacting with their corresponding counterpart functionalized small molecules.

Koh *et al*. reported fluorescence methods to provide a quantitative evaluation of vector molecules grafted on the

iron oxide nanoparticles [116]. Previous studies based on thermogravimetric and chemical analysis were used to evaluate surface modification [117-119].

5. STRUCTURAL CHARACTERIZATION

The magnetic properties of nanoparticles depend on their physical structure: their size, their shape, their microstructure, and the chemical phase or phases present. Several techniques can be used to determine the size and the chemical composition of the nanosystems. The size of the particles can be determined by transmission electron microscopy (TEM) images [120]. This technique reports the total particle size and provides details of the size distribution. Aggregates of smaller particles can be discerned.

X-ray diffraction (XRD) can be performed to obtain the crystalline structure of the particles. In a diffraction pattern, the proportion of iron oxide formed in a mixture can be quantified by comparing the intensities of an experimental peak and a reference peak. The crystal's size can be calculated also from the line broadening in the XRD pattern using the Scherrer formula [121]. Extended X-ray absorption fine structure (EXAFS) gives information on particle size, especially for small sizes [122].

Mossbauer spectroscopy is an alternative technique for assessing crystal composition. This method gives information about the order of magnitude of the Néel relaxation time, an important characteristic of superparamagnetic particles [123].

Three analytical techniques have been regularly used to characterize iron oxide superparamagnetic nanoparticles: photon correlation spectroscopy (PCS), magnetometry, and relaxivity profiles (NMRD curves) recorded over a wide range of magnetic fields. PCS measurements give a mean value of the hydrodynamic diameter of the particles [124]. Magnetometry confirms the superparamagnetic property of the particle and provides information on the specific magnetization and the mean diameter of the crystals. The fitting of the NMRD curves according to the theories [125] gives the mean crystal size, the specific magnetization, and the Néel relaxation time [126, 127].

5.1. Relaxivity and NMRD Profiles

The nuclear magnetic relaxation properties of a compound are ideally obtained by the study of its NMRD (nuclear magnetic resonance dispersion) profile, which gives the evolution of the relaxivity with respect to the external magnetic field. The relaxivity is defined as the increase of the relaxation rate of the protons of the solvent (water) induced by one millimole per liter of the active ion. For example, in the case of magnetite, the relaxivity is the relaxation rate enhancement observed for an aqueous solution containing one millimole of iron per liter.

$$R_{i(obs)} = \frac{1}{T_{i(obs)}} = \frac{1}{T_{i(diam)}} + r_i C; \quad i = 1 \text{ or } 2 \tag{2}$$

where: $R_{i(obs)}$ and $1/T_{i(obs)}$ are the global relaxation rates of the aqueous system (s^{-1}); $T_{i(diam)}$ is the relaxation time of the system before addition of the contrast agent, C is the concentration of the paramagnetic center (mmol L^{-1}), and r_i is the relaxivity (s^{-1} $mmol^{-1}$ L).

The superparamagnetic relaxation mechanism is built upon the original theory developed for paramagnetic systems. There are two contributions to proton relaxation: the innersphere and outersphere relaxations. Innersphere relaxation deals with the direct exchange of energy between protons and electrons located in the first hydration sphere of the paramagnetic ion and is dominated by dipolar and scalar coupling of the spins [128, 129]. Outersphere relaxation arises due to the movement of the water protons near the local magnetic field gradients generated by the paramagnetic ion. The interaction between proton spins and the magnetic moment is also a dipolar interaction [130].

Base of the Relaxation Theory of Superparamagnetic Colloids

The proton relaxation in superparamagnetic colloids occurs because of the fluctuations of the dipolar magnetic coupling between the nanocrystal magnetization and the proton spin. The relaxation is described by an outersphere model where the dipolar interaction fluctuates because of both the translational diffusion process and the Néel relaxation process.

This intramolecular mechanism is modulated by the translational correlation time (τ_D) that takes into account the relative diffusion constant (D) between the paramagnetic center and the solvent molecule, as well as their distance of closest approach (d). The outersphere model has been described by Freed [130].

At high magnetic high fields, the outersphere contribution is given by:

$$R_1^{os} = \frac{6400\pi}{81}\left(\frac{\mu_0}{4\pi}\right)^2 \gamma_H^2 \gamma_S^2 \hbar^2 S(S+1) NA \frac{[C]}{dD}[7j(\omega_S \tau_D) + 3j(\omega_H \tau_D)] \tag{3}$$

$$j(\omega\tau_D) = \mathrm{Re}\left[\frac{1+\frac{1}{4}\left(i\omega\tau_D + \tau_D/\tau_{S1}\right)^{1/2}}{1+\left(i\omega\tau_D + \tau_D/\tau_{S1}\right)^{1/2} + \frac{4}{9}\left(i\omega\tau_D + \tau_D/\tau_{S1}\right) + \frac{1}{9}\left(i\omega\tau_D + \tau_D/\tau_{S1}\right)^{3/2}}\right] \tag{4}$$

where d is the distance of closest approach; D is the relative molecular diffusion constant; [C] is the molar concentration of the paramagnetic ion, and $\tau_D = d^2/D$ is the translational correlation time and τ_{S1} is the electronic relaxation time.

The NMRD profiles (Fig. (**5**)) describe relaxation as a function of frequency and allow determining the correlation times that modulate the relaxation.

6. APPLICATIONS

Internalization of magnetic contrast agents is a way to label cells and to distinguish them from the surrounding tissues in magnetic resonance imaging (MRI). Thanks to their high efficacy as MRI contrast agents, superparamagnetic nanoparticles are well suited for this purpose. As mentioned earlier, they are made of an iron oxide core (one or several magnetite and/or maghemite crystals) surrounded by a stabilizing coating that can either be polymeric (polysaccharide or

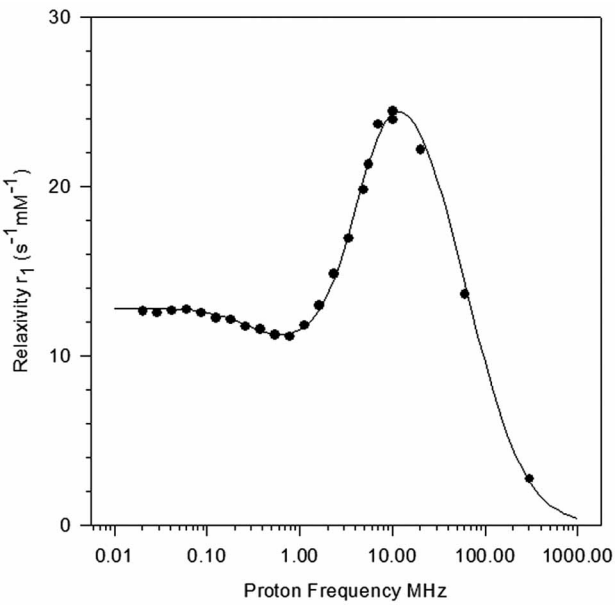

Fig. (5). Example of an NMRD profile of magnetite particles: specific magnetization (51.8 $Am^2 Kg^{-1}$) and crystal diameter (8.86 nm).

synthetic), or monomeric. Due to their capacity to shorten the T_2/T_2* relaxation time of the nuclei located in their neighborhood, they induce a signal darkening on the MR images [3]. Several categories of iron oxide particles, based on their overall (hydrodynamic) diameter, are reported in the biomedical literature: the ultrasmall particles of iron oxide (USPIO, below 50 nm), the small particles of iron oxide (SPIO, 60-180 nm), and the micron-sized particles of iron oxide (MPIO, 0.76-5.80 μm) [5, 18, 131]. Subsets of USPIO are also named: the very small iron oxide particles (VSOP, 7-9 nm) and the monocrystalline iron oxide nanoparticles (MION,~10-30 nm) [5, 18, 131-134]. The ultrasmall particles (USPIO) have a T_1 shortening power that allows them to be sometimes used as positive contrast agents [131]. It is worth noting that iron is a biocompatible ion recycled in the hemoglobin pool [18, 135].

6.1. Tissue Labeling with Iron Oxide Particles

The *in vivo* behavior of iron oxide nanoparticles is related to their binding to plasma proteins (opsonization) when injected in the circulation. This process helps to their recognition as phagocytic targets by monocytes and macrophages, mediated by specialized cell surface receptors, and to their subsequent uptake by these phagocytic cells. Opsonization is known to depend on the size, the surface charge density, and the hydrophilic/hydrophobic balance of the circulating particle; with the main observation that the smaller the size, the lower the electric charge, and the more hydrophilic the surface, the longer the particle remains in the blood [136].

Several types of superparamagnetic nanoparticles accumulate in the liver when intravenously injected. After opsonization by plasma proteins, SPIO such as Endorem® (Guerbet, Aulnay-sous-Bois, France) also named Feridex® (Berlex Inc, Montville, New Jersey, USA) coated with dextran, or Resovist® (Bayer Schering Pharma AG, Berlin, Germany) coated with carboxydextran, are phagocytosed by Kupffer cells (liver resident macrophages) within minutes. Some of these SPIO are in clinical trials or already approved for the detection of liver metastases in patients. Since they are not retained in metastases and in hepatocytes, the darkening of liver signal on T_2-weighted MR images will be observed only in healthy parts of the organ. SPIO sequestration also occurs in spleen and bone marrow macrophages, allowing detection of lesions in these areas as in the liver [5, 18, 131, 133, 137].

Sinerem® (Guerbet) also known as Combidex® (Advanced Magnetics Inc, Cambridge, Massachusetts, USA) is a dextran-stabilized USPIO. Due to their relatively small hydrodynamic diameter (20-50 nm), USPIO have a stronger T_1 relaxation as compared to SPIO, and are less likely to be captured by macrophages. As they circulate longer, they can be used as blood pool agents for T_1-weighted magnetic resonance angiography during the early phase of intravenous administration. In the later phase, USPIO accumulate in liver and spleen, but also become potent contrast agents for lymphography. Indeed, their small size enables them to reach the lymphatic system by extravasating from the blood vessels to the interstitial space. USPIO thus accumulate in lymph nodes (also *via* macrophages endocyting the nanoparticles and reaching the nodes). This distribution will be disturbed by the presence of nodal metastases, making it possible to detect with MRI the metastatic involvement of lymph nodes [5, 18, 131, 133, 136]. The biodegradation of (carboxy)dextran-coated iron oxide nanoparticles occurs in lysosomes where they accumulate subsequently to their macrophage uptake.

Several preclinical studies about toxicity, safety, biocompatibility, biodistribution, clearance and pharmacokinetics of such nanoparticular iron oxide contrast agents have been reported [138-141].

6.2. Cellular and Molecular Labeling with Iron Oxide Particles

Cellular magnetic labeling implies that cells internalize the contrast agent and become detectable by MRI. This can be accomplished *in vitro* or *in vivo* through non-specific cellular endocytosis or through pathways involving a given cell surface receptor. This latter method can thus give more specific cellular MRI results. However, iron oxide nanoparticles targeted to a cell surface molecule can also remain bound to their target, being useful as molecular MRI probes. In a majority of reported cases, iron oxide particles used as intracellular magnetic tags were well tolerated by cells and were not deleterious for cell viability [5, 131, 133, 142].

6.2.1. Intracellular Trapping of Iron Oxide Nanoparticles through Non-Specific Internalization Pathways

A non-specific magnetic labeling means that the loading of cells with iron oxide nanoparticles occurs passively, *via* mechanisms of endocytosis that are mainly not receptor-dependent, such as fluid-phase endocytosis. Nowadays, the goal to achieve in many studies is the non-invasive *in vivo* MRI monitoring of cells that are potentially useful for cell therapy. In this context, cells of interest have to be magnetically labeled in culture prior to their *in vivo* implantation, often with iron oxide nanoparticles, and, for many of them, without having a professional phagocytic function.

Undifferentiated (stem) or less differentiated (progenitor) cells that could differentiate to replace dead cells in a damaged organ and even, in some cases, migrate to the injured area have been transplanted in several animal models of diseases [5, 131, 133]: central nervous system (spinal cord injury and cerebral stroke) [143], heart (myocardial infarction) [144, 145], kidneys (nephropathy, ischemia/reperfusion) [146], and liver (CCl_4-induced centrolobular liver necrosis) [147].

In the field of cell-based anti-cancer therapies, the tumoral targeting of adequately antigen-sensitized iron oxide nanoparticle-labeled lymphocytes (e.g. splenocytes, T-cells) [148, 149] and the tumoral tropism of mesenchymal stem cells [150] could also be monitored by MRI. *In vitro* prelabeled endothelial progenitor cell incorporation in the neovessels of implanted tumors has been MR imaged [133]. In the current cellular MRI field, an *in vitro* iron oxide prelabeling of true phagocytic cells is not very frequent: in immune cell-based cancer therapies, monocytes/macro-phages have been used for tumor targeting in an animal model of glioma or for infarcted heart repairing improvement [151], and dendritic cells have been monitored after intra-nodal implantation in melanoma patients [133]. The behavior of cultured non-phagocytic cells regarding iron oxide nanoparticles is an important aspect to study and understand. For example, several effects induced on fibroblasts by homemade USPIO used as intracellular magnetic tags of these cells have been reported [152]. Fibroblasts appeared to largely internalize dextran-coated nanoparticles. Cell morphology modifications (disrupted membrane areas) due to rearrangement of cytoskeletal elements, and an increase of clathrin levels at the cell peripheries suggested a fluid-phase endocytosis of the nanoparticles [153].

Commercially available SPIO are often used to label cells: rat bone marrow mesenchymal cells, mouse embryonic stem cells, and hematopoietic progenitor cells have been incubated with SPIO coated by neutral dextran (i.e., Endorem® or Feridex®) [143], and human mesenchymal stem cells have been labeled with ionic carboxydextran-coated SPIO (Resovist®) [153]. Indeed, it has been shown that, as for phagocytic cells (i.e., monocytes or macrophages) [154], SPIO are accumulated more efficiently than USPIO by cells having no professional phagocytic function [155]. Furthermore, the presence of charged molecules at the nanoparticle surface has been found to improve the intracellular magnetic labeling of many cell types. In several studies, the cellular uptake of ferumoxides was optimized by mixing the superparamagnetic contrast agent with a cationic transfection agent, which usually helps to deliver DNA into cells. Positively charged complexes formed by ferumoxides and poly-L-lysine (PLL), protamine sulfate or Superfect™ adsorb on the negatively charged cell surface, which facilitates their encapsulation in endosomes [5, 131, 133]. The same approach has been developed with cationic transfection liposomes (such as Lipofectamine™ or FuGENE™), which were mixed with several types of SPIO or USPIO to improve the cellular magnetic labeling with these nanoparticles [5, 131, 133, 155]. Magnetoelectroporation has allowed achieving an instant cellular magnetic labeling with ferumoxides [133]. Arginine-containing peptides have "cell penetration" properties and help to deliver biological molecules into cells [156]. A well known example is the highly cationic peptide derived from the basic (arginine-rich) domain of the transactivator of transcription (Tat) protein of the human immunodeficiency virus (HIV) [133]. Superparamagnetic contrast agents have been linked to this Tat peptide to facilitate their cellular uptake [5, 18, 133]. Tat-conjugated cross-linked iron oxides (CLIO-Tat) allowed achieving a six-fold higher iron loading of human neural stem cells than CLIO-NH_2 particles, which were more efficient than Feridex®, the weakest being MION. With PLL, the three latter were found to have similar tagging properties as CLIO-Tat [157]. Iron oxide nanoparticles with a carboxylated, thus anionic, coating also have allowed a more efficient magnetic labeling of cultured non-phagocytic cells than nanoparticles coated by a neutral polymer, although the uptake mechanisms remain unknown or hypothetical [5, 131, 158, 159] (Fig. (**6**)). It is interesting to note that similar observations were reported with monocytes [160]. In cell therapy experiments aiming at curing Type 1 diabetes, magnetically labeled pancreatic islets [161, 162] were subsequently transplanted in the liver of diabetic rats or mice through injection in the portal vein and visualized by MRI. The achievement of a sufficient contrast requires the endocytosis of millions of SPIO or USPIO, and cell division can dilute the label beyond the detection threshold. As compared to nanometer-sized particles, some advantages have been found in the use of micron-sized particles of iron oxide (MPIO) to label cells. The possibility to MR image labeled cells by detecting single fluid-phase endocytosed MPIOs indeed overcame the problems related to the dilution of the magnetic label induced by the cell divisions. Furthermore, MPIO, such as those from Bangs Laboratories (Fishers, Indiana, USA), coated with an inert polymer (styrene/divinyl benzene) cannot be degraded within the cell, which is not the case with dextran [131]. The *in vivo* detectability of transplanted MPIO-labeled mouse hepatocytes as single cells has also been reported [163].

Iron oxide nanoparticles used as intracellular (endosomal) magnetic tags are not toxic since no significant decrease of cell viability is reported in a majority of cases, even at long term [5, 18, 131, 133]. Nevertheless, several observations tend to suggest a deleterious effect of high intracellular iron levels, especially when this excess iron is in ferrous state and free to enter reactions generating free radicals, such as the Fenton reaction producing hydroxyl radicals that can react with cellular components and cause lethal oxidative damage. A Feridex®-PLL labeling of MSCs (mesenchymal stem cells) allowed reaching an iron content of 550 pg/cell, but the percentage of dead cells after incubation was 43%, which was significantly higher than for the unlabeled control cells (±15%). MSCs containing approximately 50 pg of iron/cell had a normal viability [164]. In a report studying the Feridex®-labeling of rabbit myoblasts, it was found that these SPIO were significantly less harmful for the cells when mixed with cationic liposomes, although at similar intracellular iron concentrations. No generation of free radicals occurred with the SPIO-liposome complex, which was also not easily biodegraded [5, 131, 165]. The risk of oxidative stress due to a possible release of iron in the cytoplasm after lysosomal dissolution of iron oxide nanoparticles is thus to be considered at high intracellular loading. The looseness or stability of the molecules coating the iron oxide crystals of-

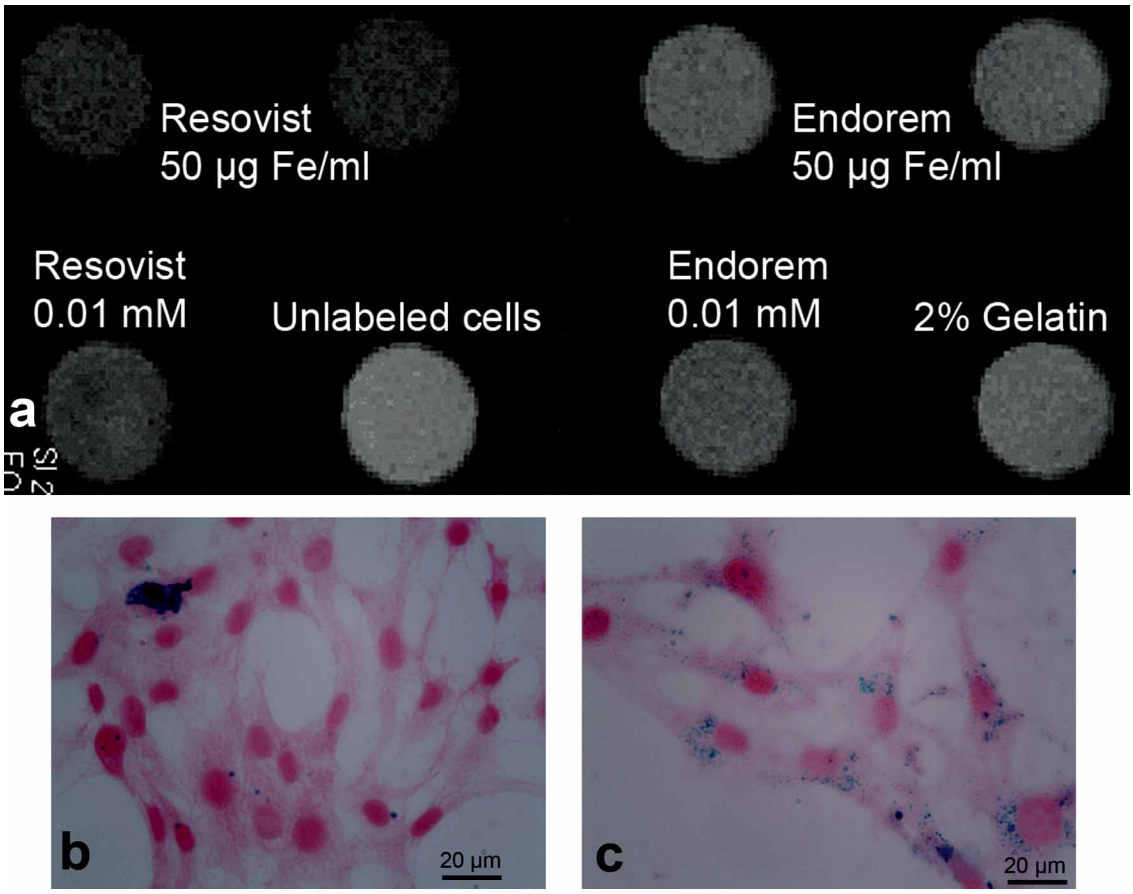

Fig. (6). (**a**) T_2-weighted MR images (TR/TE: 3000/15 ms, 16th echo (240 ms), 5x10^5 cells/ml in 2% gelatin) of 3T6 fibroblasts after 48 hours of SPIO labeling with 50 µg Fe/ml of Endorem® or Resovist®. (**b** & **c**) Cytochemical staining of iron associated to 3T6 fibroblasts after 48 hours of SPIO labeling with 50 µg Fe/ml of Endorem® (**b**) or Resovist® (**c**), shown at original magnification Gx40 [159].

ten by adsorption can also be important in the context of (U)SPIO intracellular labeling [134]. Cells also react at the level of their iron metabolism and storage. After labeling with SPIO-protamine sulfate complexes, non-phagocytic cells have been found to decrease their transferrin receptor levels (involved in iron uptake) during the first week post-incubation and increase their ferritin (involved in iron storage) expression until at least one month post-labeling in the case of MSCs, which also kept comparable iron contents for this period as slowly dividing cells [133, 166]. It has to be noted that specialized cells (e.g., macrophages) handle large intracellular iron concentrations differently to the usually studied non-phagocytic cells of interest (e.g., because of their higher level of antioxidative molecules or their ability to excrete excess iron) [134, 165]. From the oxidative stress viewpoint, MPIO have been presented as less risky thanks to their inertness to cell polymer coating, however raising the question of how these particles can be cleared from cells [131, 133].

A direct *in vivo* non-specific labeling of cells with iron oxide particles requires a sufficient cellular uptake of the MRI contrast agent, provided by the blood circulation after intravenous administration or injected *in situ*. As inflammatory diseases are associated to a monocyte/macrophage activity, the same macrophage targeting approach as that allowing MRI lymphography with USPIO or liver tumor characterization with SPIO has been further developed to visualize inflammatory lesions in living organisms including humans. Following intravenous injection of iron oxide particles (mainly USPIO [5, 18, 131, 167-173] but also SPIO [5, 131, 174, 175] and MPIO [133, 176]), macrophage infiltration during inflammatory events can be visualized by MRI (e.g. in multiple sclerosis [5, 18, 131, 166, 169, 171], arthritis [5, 131, 170], cerebral stroke [5, 18, 131, 168, 169, 171, 175], graft rejection [5, 18, 131, 133, 174, 176], nephropathies [5, 131], atherosclerotic plaques [5, 18, 131, 169] and tumors [18, 143, 169, 171-173]). It has to be noted that macrophage labeling with iron oxide nanoparticles depends on cell surface receptors. *In vitro* studies indeed have reported a role of the scavenger receptor A in the uptake of dextran-coated SPIO by mouse peritoneal macrophages [154]. The USPIO labeling of monocytes has been found to be mediated by the Mac-1 integrin, independently of the nanoparticle surface coating, but dependently of the activation status of the integrin, which is in a high-affinity state on activated monocytes [177].

The passive targeting of tumors by long circulating MION and USPIO occurs *via* extravasation of the nanoparticles through the leaky tumoral capillaries, as observed in animal models. Their interstitial accumulation thus allows cellular magnetic labeling, mainly at the tumor margin. Tumor-associated macrophages, reactive astrocytes, neuroglial

fibrous scar (in brain tumor models), and even sometimes tumor cells themselves have been reported to uptake the nanoparticles [18, 172, 173]. Magnetic labeling of tumor-associated cells (macrophages, fibroblasts, endothelial cells) has been achieved also by magnetically targeting liposomes loaded with iron oxide nanoparticles to tumors implanted in mice. A preferential accumulation of these polyethyleneglycol-coated long-circulating magnetoliposomes (200 nm in diameter) has been induced by placing a magnet to the skin above the tumor during the circulation of the intravenously injected iron oxides. Magnetoliposomes have been magnetically driven to the tumor more efficiently than non-encapsulated USPIO. As for these latter, the mechanism of tumoral accumulation of magnetoliposomes is diffusion to the interstitium, through the leaky vasculature in the most highly vascularized zone. An *in vivo* magnetic labeling of non-phagocytic cells has been achieved after *in situ* injection of iron oxide particles [178].

Neural progenitor cells of the subventricular zone of the rodent brain have been magnetically labeled thanks to an uptake of MPIO injected into the anterior right lateral ventricle. Their migration towards the olfactory bulb was monitored by MRI [179]. MION have been conjugated to the lectin wheat germ agglutinin, so that they could be transported *via* slow axonal transport by the guinea pig facial nerve, or the rat sciatic nerve, after direct injection into these peripheral nerves [180, 181]. A non-specific uptake of dextran-coated MION in neurons after delivery of the nanoparticles in the rat brain has also been reported [182].

6.2.2. Intracellular Trapping of Iron Oxide Nanoparticles through Interaction with a Cell Surface Receptor

The targeting of cell surface molecules with adequately modified iron oxide particles has allowed cellular delivery of the magnetic tag and MR imaging of specific cell types [5, 18, 131, 133]. Cells overexpressing the transferrin receptor or the folate receptor have been loaded with particles conjugated to the respective ligands of these molecules [5, 18, 131, 133, 183, 184]. Since the overexpressed transferrin and folate receptors are characteristic of several cancer cell types, they have been targeted with iron oxide nanoparticles for MR imaging of tumors [183] or with the aim of finding a tumor cell-specific mediator of intracellular magnetic hyperthermia (nanoparticles heating under the influence of an alternating magnetic field) [184].

Non-invasive lymphocyte imaging has been attempted. T-cells infiltrating the brain of mice infected with Theiler's encephalomyelitis virus and of mice with autoimmune encephalomyelitis have been labeled *in vivo* with intravenously injected iron oxide nanoparticles conjugated to antibodies directed against CD8 and CD4 antigens [185]. During Type 1 diabetes progression, $CD8^+$ T-cells invading the pancreas and destroying the pancreatic islets of non-obese diabetic mice have been specifically targeted with iron oxide nanoparticles. The magnetic tags bore a mimotope of the islet surface molecule recognized by the main histocompatibility complex of the autoreactive lymphocytes [186].

The $\alpha_v\beta_3$ integrin is a well-known tumor angiogenesis marker expressed on the surface of endothelial cells in neovessels. This molecule has been successfully targeted on endothelial cell cultures and in angiogenic mouse-implanted tumors, with USPIO conjugated to the Arg-Gly-Asp (RGD) peptide [187]. RGD-conjugated nanoparticles also have been reported to label $\alpha_v\beta_3$-expressing tumor cells *in vitro* and *in vivo* [188].

Tumor cells expressing the membrane-bound matrix metalloproteinase MMP-2 can also be labeled with iron oxide nanoparticles conjugated to a peptide: the 36 amino acid chlorotoxin. This MMP-2 ligand has allowed to target polyethyleneglycol-coated iron oxide nanoparticles to a 9L gliosarcoma cell line in culture or implanted as a xenograft tumor *in vivo* [189]. It should be reminded that a hydrophilic polymer such as polyethyleneglycol (PEG) helps to reduce the opsonization by plasma proteins and the subsequent macrophage uptake of the nanoparticles, which can thus remain longer in the blood circulation [190].

Iron oxide nanoparticles have been bound also to hormones (luteinizing hormone releasing hormone (LHRH) and chorionic gonadotropin (betaCG)) in order to label cultured human breast cancer cells. *In vivo*, implanted breast tumors and their metastases in the lungs have been successfully labeled with LHRH-bound nanoparticles [191].

The avidin/biotin system has been used also to specifically target cancer cells with iron oxide nanoparticles. A labeling of prostate cancer cells has been achieved using a biotinylated anti-prostate-specific membrane antigen (PSMA) bound to streptavidin-labeled iron oxide nanoparticles [192].

Targeting phosphatidylserine on the outer leaflet of the membrane of cells undergoing apoptosis is an often used way to MR image the programmed cell death process. Externalization of phosphatidylserine is a feature of lipid-loaded (foamy) macrophages in high grade atherosclerotic lesions. Their staining with annexin V-conjugated iron oxide nanoparticles has allowed an MRI evaluation of vulnerable plaques in hyperlipidemic rabbits [193].

Endothelial markers of pathologies have been targeted also with iron oxide nanoparticles (e.g., vascular adhesion molecule-1 (VCAM-1) and E-Selectin, which play a critical role in the leukocyte-endothelial adhesion taking place during inflammatory phenomena). A peptide binding VCAM-1 and conjugated to nanoparticles has allowed the detection of cells expressing this adhesion molecule in acute inflammatory and atherosclerotic *in vivo* mouse models [18]. Expression of E-selectin has been imaged in an *in vivo* model by labeling cytokine (interleukin-1β)-stimulated human umbilical vein endothelial cells (HUVECs) with iron oxide nanoparticles conjugated to a high affinity anti-human E-selectin antibody fragment [194].

6.2.3. Iron Oxide Nanoparticles as Molecular MRI Probes

The targeting of cell surface molecules with iron oxide nanoparticles has also been reported [18, 143]. The Her-2/Neu receptor expressed by breast cancer cells has been MR imaged with prelabeled cells incubated with the adequate monoclonal antibody and subsequently with streptavidin-conjugated iron oxide nanoparticles [18]. After incubation with a biotinylated pan T-cell anti-CD5 antibody, peripheral lymphocytes have been labeled *in vitro*, mainly extracellularly, using streptavidin-coated MPIO [195]. To target apop-

totic cells, iron oxide nanoparticles have been conjugated to molecules recognizing phosphatidylserine, such as the C2 fragment of synaptotagmin or annexin-V [18, 143].

In a recent work, a cationic transfection agent (protamine sulfate) conjugated to annexin-V has been used to decorate anionic citrate-coated iron oxide nanoparticles (VSOP) through electrostatic interactions. The obtained target-specific nanoparticle has been successfully tested on apoptotic human lymphoblastic T cell (Jurkat) cultures and its small size (~15 nm) is interesting for *in vivo* applications since it allowed them to extravasate to reach their target [196].

To target endothelial markers of inflammation, anti-VCAM-1 antibodies have been conjugated to MPIO, allowing an *in vivo* detection of VCAM-1 expression in a mouse model of acute brain inflammation [197]. MPIO conjugated to both anti-P-selectin and anti-VCAM-1 antibodies were shown to bind to the endothelium of the atherosclerosis-presenting aortic root of mice. MRI detection of the particles has been however only possible *ex vivo* [198]. Using a method based on the well-known ELISA (enzyme-linked immunosorbent assay), the specificity of integrin-targeted USPIO (conjugated to the connecting segment-1 fragment of fibronectin, the peptide GRGD, or a non-peptidic RGD mimetic) has been quantitatively evaluated by MRI on stimulated Jurkat cells [6]. A synthetic mimetic of sialyl-Lewis^X (sLe^X, E-selectin's natural ligand), covalently bound to the dextran coating of USPIO, has been successfully tested on HUVECs expressing E-selectin after stimulation with the cytokine tumor necrosis factor-alpha (TNF-alpha) [7] (Fig. (**7**)).

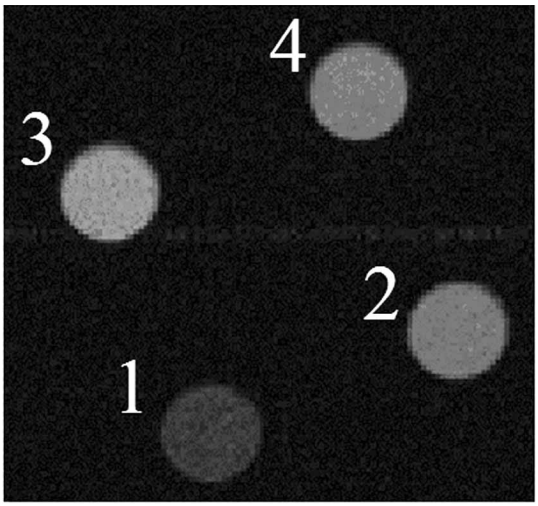

Fig. (7). Axial spin echo T_2-weighted MR Image of HUVECs ($2x10^7$ cells/ml in 2% gelatin). 1: TNF-α stimulated + 4 mM USPIO-g-sLe^x, 2: unstimulated + 4 mM USPIO-g-sLe^x, 3: TNF-α stimulated + 4 mM ungrafted USPIO, 4: unstimulated + 4 mM ungrafted USPIO.

7. CONCLUSIONS

Iron oxide nanoparticles have been used for many years in the MRI field of biomedical research. Basically, two categories of particles, originally used as intravenously-injected MRI contrast agents, can be discriminated based on their overall size. Larger ones were approved for liver imaging since their Kupffer cell uptake occurs after a short circulation time. Smaller ones, having an ability to partially escape this early hepatic clearance mechanism, can undergo macrophage uptake in less accessible areas. The circulation time properties of a particle are related to the following parameters: the smaller its size, the more neutral and hydrophilic its surface, the longer it remains in the blood [136].

The way in which these smaller and larger particles are used in the cellular magnetic labeling field roughly reflects the properties they have in the blood stream. Larger particles or particles displaying a non-neutral surface (thanks to their coating or to a transfection agent they are mixed with) are efficient tools for magnetic labeling of cultured cells, although these cells have no professional phagocytic function. Labeled cells can then be transplanted and monitored by MRI in a broad spectrum of applications. Direct *in vivo* magnetic labeling of cells is mainly (but not exclusively) performed by intravenous injection of long-circulating iron oxide-based MRI contrast agents, which can extravasate and/or undergo an uptake by macrophages in a sufficient amount in areas of interest such as inflamed regions or tumors. Particles with long circulation times (i.e., USPIO, VSOP), or able to induce a strong T_2* effect individually (e.g., MPIO) have been modified also by conjugation to a ligand, so that their cellular uptake, or at least their binding to the cell surface, could occur through a specific ligand-receptor interaction, *in vivo* as well as *in vitro*. Thus, experimentally as well as in a few trials on humans, iron oxide particles currently find promising applications.

ACKNOWLEDGEMENTS

The authors thank Mrs. Patricia de Francisco for her help in preparing the manuscript. This work was supported by the FNRS, the PAI and the ARC Program 05/10-335 of the French Community of Belgium. The support and sponsorship concerted by COST Action D38 and EMIL program are kindly acknowledged.

REFERENCES

[1] Jain, T.K.; Reddy, M.K.; Morales, M.A.; Leslie-Pelecky, D.L.; Labhasetwar, V. Biodistribution, clearance, and biocompatibility of iron oxide magnetic nanoparticles in rats. *Mol. Pharm.,* **2008**, *5(2)*, 316-327.

[2] Chourpa, I.; Douziech-Eyrolles, L.; Ngaboni-Okassa, L.; Fouquenet, J.F.; Cohen-Jonathan, S.; Souce, M.; Marchais, H.; Dubois, P. Molecular composition of iron oxide nanoparticles, precursors for magnetic drug targeting, as characterized by confocal Raman microspectroscopy. *Analyst*, **2005**, *130(10)*, 1395-1403.

[3] Laurent, S.; Forge; D.; Port, M.; Roch, A.; Robic, C.; Vander Elst, L.; Muller, R.N. Magnetic iron oxide nanoparticles: synthesis, stabilization, vectorization, physico-chemical characterizations and biological applications. *Chem. Rev*., **2008**, *108(6)*, 2064-2110.

[4] Bulté, J.W. Intracellular endosomal magnetic labeling of cells. *Methods Mol. Med.,* **2006**, *124*, 419-439.

[5] Modo, M.; Hoehn, M.; Bulté, J.W. Cellular MR imaging. *Mol. Imaging*, **2005**, *4(3)*, 143-164.

[6] Burtea, C.; Laurent, S.; Vander Elst, L.; Muller, R.N. C-MALISA (Cellular Magnetic-Linked Immunosorbent Assay), a new application of cellular ELISA for MRI. *J. Inorg. Biochem*., **2005**, *99(5)*, 1135-1144.

[7] Boutry, S.; Laurent, S.; Vander Elst, L.; Muller, R.N. Specific E-selectin targeting with a superparamagnetic MRI contrast agent. *Contrast Med. Mol. Imaging*, **2006**, *1(1)*, 15-23.

[8] Gupta, A.K.; Gupta, M. Synthesis and surface engineering of iron oxide nanoparticles for biomedical applications. *Biomaterials*, **2005**, *26(18)*, 3995-4021.

[9] Chastellain, M.; Petri, A.; Gupta, A.; Rao, K.V.; Hofmann, H. Superparamagnetic silica-iron oxide nanocomposites for application in hyperthermia. *Adv. Eng. Mater.*, **2004**, *6(4)*, 235-241.

[10] Murthy S.K. Nanoparticles in modern medicine: state of the art and future challenges. *Int. J. Nanomed*., **2007**, *2(2)*, 129-141.

[11] Douziech-Eyrolles, L.; Marchais, H.; Hervé, K.; Munnier, E.; Soucé, M.; Linassier, C.; Dubois, P.; Chourpa, I. Focalisation magnétique d' agents anticancéreux. *Int. J. Nanomed*., **2007**, *2(4)*, 541-550.

[12] Willard, M.A.; Kurihara, L.K.; Carpenter, E.E.; Calvin, S.; Harris, V.G. Chemically Prepared Magnetic Nanoparticles. *Encyclopedia of Science and Nanotechnology*, Ed. by H.S. Nalwa, **2004**, *1*, 815-848.

[13] Tavakoli, A.; Sohrabi, M.; Kargari, A. A review of methods for synthesis of nanostructured metals with emphasis on iron compounds. *Chem. Pap*., **2007**, *61(3)*, 151-170.

[14] Majewski, P.; Thierry, B. Functionalized magnetite nanoparticles-synthesis, properties, and bio-applications. *Crit. Rev. Solid State Mater.*, **2007**, *32(3-4)*, 203-215.

[15] Jeong, U.; Teng, X.; Wang, Y.; Yang, H.; Xia, Y. Superparamagnetic colloids: controlled synthesis and niche applications. *Adv. Mater*., **2007**, *19*, 33-60.

[16] Wang, Y.X.; Hussain, S.M.; Krestin, G.P. Superparamagnetic iron oxide contrast agents: physicochemical characteristics and applications in MR imaging. *Eur. Radiol.*, **2001**, *11*, 2319-2331.

[17] Bulte, J.W.; Kraitchman, D.L. Iron oxide MR contrast agents for molecular and cellular imaging. *NMR Biomed*., **2004**, *17*, 484-499.

[18] Thorek, D.L.; Chen, A.K.; Czupryna, J.; Tsourkas, A. Iron oxide nanoparticle probes for molecular imaging. *Ann. Biomed. Eng.*, **2006**, *34*, 23-38.

[19] Papell, S.S.; Faber, O.C. On the influence of nonuniform magnetic fields on ferromagnetic colloidal sols. *NASA Technical Note*, report number NASA-TN-D-4676, Glenn Research Center, Washington, **1968**, pp. 1-25.

[20] Massart, R. Preparation of aqueous magnetic liquids in alkaline and acidic media. *IEEE Trans. Magn*., **1981**, *17*, 1247-1248.

[21] Massart, R.; Dubois, E.; Cabuil, V.; Hasmonay, E. Preparation and properties of monodisperse magnetic fluids. *J. Magn. Magn. Mater.*, **1995**, *149(1-2)*, 1-5.

[22] Liu, X.; Ma, Z.; Xing, J.; Liu, H. Preparation and characterization of amino–silane modified superparamagnetic silica nanospheres. *J. Magn. Magn. Mater.*, **2004**, *270(1-2)*, 1-6.

[23] Mornet, S.; Portier, J.; Duguet, E. A method for synthesis and functionalization of ultrasmall superparamagnetic covalent carriers based on maghemite and dextran. *J. Magn. Magn. Mater.*, **2005**, *293(1)*, 127-134.

[24] Duguet, E.; Mornet, S.; Portier, J. Ferrofluids stable in neutral media and ferrofluids employing surface-modified particles. French patent FR2855315, PCT *WO2004107368*.

[25] Mornet, S.; Vasseur, S.; Grasset, F.; Duguet, E. Magnetic nanoparticle design for medical diagnosis and therapy. *J. Mater. Chem.*, **2004**, *14*, 2161-2175.

[26] Woo, K.; Hong, J.; Ahn, J.-P. Synthesis and surface modification of hydrophobic magnetite to processible magnetite@silica-propylamine. *J. Magn. Magn. Mater.*, **2005**, *293(1)*, 177-181.

[27] Zheng, Y.-H.; Cheng, Y.; Bao, F.; Wang, Y.-S. Synthesis and magnetic properties of Fe_3O_4 nanoparticles. *Mater. Res. Bull.*, **2006**, *41(3)*, 525-529.

[28] Sun, S.; Zeng, H.; Robinson, D.B.; Raoux, S.; Rice, P.M.; Wang, S.X.; Li, G. Monodisperse MFe_2O_4 (M = Fe, Co, Mn) nanoparticles. *J. Am. Chem. Soc*., **2004**, *126(1)*, 273-279.

[29] Park, J.; An, K.; Hwang, Y.; Park, J.-G.; Noh, H.-J.; Kim, J.-Y.; Park, J.-H.; Hwang, N.-M.; Hyeon, T. Ultra-large-scale syntheses of monodisperse nanocrystals. *Nat. Mater*. **2004**, *3(12)*, 891-895.

[30] Dresco, P.A.; Zaitsev, V.S.; Gambino, R.J.; Chu, B. Preparation and properties of magnetite and polymer magnetite nanoparticles. *Langmuir*, **1999**, *15(6)*, 1945-1951.

[31] O'Connor, C.J.; Seip, C.; Sangregorio, C.; Carpenter, E.; Li, S.; Irvin, G.; John, V.T. Nanophase magnetic materials: synthesis and properties. *Mol. Cryst. Liq. Cryst.*, **1999**, *335*, 1135-1154.

[32] Santra, S.; Tapec, R.; Theodoropoulou, N.; Dobson, J.; Hebard, A.; Tan, W. Synthesis and characterization of silica-coated iron oxide nanoparticles in microemulsion: the effect of nonionic surfactants. *Langmuir*, **2001**, *17*, 2900–2906.

[33] Liz, L.; Lopez-Quintela, M.A.; Mira, J.; Rivas, J. Preparation of colloidal Fe3O4 ultrafine particles in microemulsions. *J. Mater. Sci.*, **1994**, *29(14)*, 3797-3801.

[34] Meldrum, F.C.; Heywood, B.R.; Mann, S. Magnetoferritin: *in vitro* synthesis of a novel magnetic protein. *Science*, **1992**, *257*, 522-523.

[35] Dickson, D.P.E.; Walton, S.A.; Mann, S.; Wong, K. Properties of magnetoferritin: a novel biomagnetic nanoparticle. *Nanostruct. Mater.*, **1997**, *9*, 595-598.

[36] Sangregorio, C.; Wiemann, J.K.; O'Connor, C.J.; Rosenzweig, Z. A new method for the synthesis of magnetoliposomes. *J. Appl. Phys.*, **1999**, *85(8)*, 5699-5701.

[37] De Cuyper, M.; Joniau, M. Mechanistic aspects of the adsorption of phospholipids onto lauric acid stabilized magnetite nanocolloids. *Langmuir*, **1991**, *7(4)*, 647-652.

[38] Pileni, M.P.; Duxin, N. Micelle technology for magnetic nanosized alloys and composites. *Chem. Innov.*, **2000**, *30(2)*, 25-33.

[39] Inouye, K.; Endo, R.; Otsuka, Y.; Miyashiro, K.; Kaneko, K.; Ishikawa, T. Oxygenation of ferrous ions in reversed micelle and reversed microemulsion. *J. Phys. Chem*., **1982**, *86(8)*, 1465-1469.

[40] Verelst, M.; Ely, T.O.; Amiens, C.; Snoeck, E.; Lecante, P.; Mosset, A.; Respaud, M.; Broto, J.M.; Chaudret, B. Synthesis and characterization of CoO, Co_3O_4, and mixed Co/CoO nanoparticles. *Chem. Mater.*, **1999**, *11(10)*, 2702-2708.

[41] Puntes, V.F.; Krishnan, K.M.; Alivisatos, A.P. Synthesis of colloidal cobalt nanoparticles with controlled size and shapes. *Top. Catal.*, **2002**, *19(2)*, 145-148.

[42] Rotstein, H.G.; Tannenbaum, R. J. Cluster coagulation and growth limited by surface interactions with polymers. *Phys. Chem. B*., **2002**, *106(1)*, 146-151.

[43] Ely, T.O.; Amiens, C.; Chaudret, B.; Snoeck, E.; Varest, M.; Respaud, M.; Broto, J.M. Synthesis of nickel nanoparticles. Influence of aggregation induced by modification of poly(vinylpyrrolidone) chain length on their magnetic properties. *Chem. Mater.*, **1999**, *11(3)*, 526-529.

[44] Sidorov, S.N.; Bronstein, L.M.; Davankov, V.A.; Tsyurupa, M.P.; Solodovnikov, S.P.; Valetsky, P.M.; Wilder, E.A.; Spontak, R.J. Cobalt nanoparticle formation in the pores of hyper-cross-linked polystyrene: control of nanoparticle growth and morphology. *Chem. Mater*., **1999**, *11(11)*, 3210-3215.

[45] Park, S.J.; Kim, S.; Lee, S.; Khim, Z.G.; Char, K.; Hyeon, T. Synthesis and magnetic studies of uniform iron nanorods and nanospheres. *J. Am. Chem. Soc.*, **2000**, *122*, 8581-8582.

[46] Lee, C.M.; Jeong, H.J.; Kim, S.L.; Kim, E.M.; Kim, D.W.; Lim, S.T.; Jang, K.Y.; Jeong, Y.Y.; Nah, J.W.; Sohn, M.H. SPION-loaded chitosan-linoleic acid nanoparticles to target hepatocytes. *Int. J. Pharm.*, **2008**, *371(1-2)*, 163-169.

[47] Bae, K.H.; Ha, Y.J.; Kim, C.; Lee, K.R.; Park, T.G. Pluronic/chitosan shell cross-linked nanocapsules encapsulating magnetic nanoparticles. *J. Biomater. Sci. Polym. Ed*., **2008**, *19(12)*, 1571-1583.

[48] Kaushik, A.; Khan, R.; Solanki, P.R.; Pandey, P.; Alam, J.; Ahmad, S.; Malhotra, B.D. Iron oxide nanoparticles-chitosan composite based glucose biosensor. *Biosens. Bioelectron.*, **2008**, *24(4)*, 676-683.

[49] Jun, Y.W.; Jang, J.T.; Cheon, J. Magnetic nanoparticle assisted molecular MR imaging. *Adv Exp. Med. Biol*., **2007**, *620*, 85-106.

[50] Roque, A.C.; Bicho, A.; Batalha, I.L.; Cardoso, A.S.; Hussain, A. Biocompatible and bioactive gum Arabic coated iron oxide magnetic nanoparticles. *J. Biotechnol.*, **2009**, in press.

[51] Sosnovik, D.E.; Nahrendorf, M.; Weissleder, R. Magnetic nanoparticles for MR imaging: agents, techniques and cardiovascular applications. *Basic Res. Cardiol.*, **2008**, *103(2)*, 122-130.

[52] Hyeon, T.; Lee, S.S.; Park, J.; Chung, Y.; Na, H.B. Synthesis of highly crystalline and monodisperse maghemite nanocrystallites without a size-selection process. *J. Am. Chem. Soc*., **2001**, *123(51)*, 12798-12801.

[53] Suslick, K.S.; Hyeon, T.; Fang, M. Nanostructured materials generated by high-intensity ultrasound: sonochemical synthesis and catalytic studies. *Chem. Mater.*, **1996**, *8(8)*, 2172-2179.

[54] Bellissent, R.; Galli, G., Hyeon, T.; Migliardo, P.; Parette, G.; Suslick, K.S. Magnetic and structural properties of amorphous transition metals and alloys. *J. Non-Cryst. Solids*, **1996**, *205-207*, 656-659.

[55] Shafi, K.V.P.M.; Gedanken, A.; Goldfarb, R.B.; Felner, I. Sonochemical preparation of nanosized amorphous Fe-Ni alloys. *J. Appl. Phys.*, **1997**, *81*, 6901-6905.

[56] Kataby, G.; Prozorov, T.; Koltypin, Y.; Cohen, H.; Sukenik, C.N.; Ulman, A.; Gedanken, A. Self-assembled monolayer coatings on amorphous iron and iron oxide nanoparticles: thermal stability and chemical reactivity studies. *Langmuir*, **1997**, *13*, 6151-6158.

[57] Ramesh, S.; Cohen, Y.; Aurbach, D.; Gedanken, A. Atomic force microscopy investigation of the surface topography and adhesion of nickel nanoparticles to submicrospherical silica. *Chem. Phys. Lett.*, **1998**, *287(3-4)*, 461-467.

[58] Shafi, K.V.P.M.; Ulman, A.; Yari, X.; Yang, N.L.; Estournes, C.; White, H.; Rafailovich, M. Sonochemical synthesis of functionalized amorphous iron oxide nanoparticles. *Langmuir*, **2001**, *17(16)*, 5093-5097.

[59] Vijaya Kumar, R.; Diamant, Y.; Gendanken, A. Sonochemical synthesis and characterization of nanometer-size transition metal oxides from metal acetates. *Chem. Mater.*, **2000**, *12(8)*, 2301-2305.

[60] Dai, Z.; Meiser, F.; Möhwald, H. Nanoengineering of iron oxide and iron oxide/silica hollow spheres by sequential layering combined with a sol–gel process. *J. Colloid Interface Sci.*, **2005**, *288(1)*, 298-300.

[61] Durães, L.; Costa, B.F.O.; Vasques, J.; Campos, J.; Portugal, A. Phase investigation of as-prepared iron oxide/hydroxide produced by sol–gel synthesis. *Mater. Lett.*, **2005**, *59(7)*, 859-863.

[62] Brinker, C.J.; Sherrer, G.W. In: *Sol-gel science*, Academic Press, New York, **1990**.

[63] Raileanu, M.; Crisan, M.; Petrache, C.; Crisan, D.; Jitianu, A.; Zaharescu, M.; Predoi, D.; Kuncser, V.; Filoti, G. Sol-Gel Fe_xO_y-SiO_2 nanocomposites. *Rom. J. Phys.*, **2005**, *50 (5-6)*, 595-606.

[64] Wilard, M.A.; Kurihara, L.K.; Carpenter, S.E.; Calvin, S.; Harris, V.G. Chemically prepared magnetic nanoparticles. *Int. Mater. Rev.*, **2004**, *49(3-4)*, 125-170.

[65] Cai, W.; Wan, J. Facile synthesis of superparamagnetic magnetite nanoparticles in liquid polyols. *J. Colloid Inter. Sci.*, **2007**, *305*, 366-370.

[66] Reetz, M.T.; Helbig, W.; Quasick, S.A. Electrochemical Methods in the Synthesis of Nanostructured Transition Metal Clusters. in: « Active Metals, Preparation, Characterization, Applications », (A. Furster, Ed) VCH, Weinheim, **1996**, 279-297.

[67] Pascal, C.; Pascal, J.L.; Favier, F.; Elidrissi Moubtassim, M.L.; Payen, C. Electrochemical synthesis for the control of γ-Fe_2O_3 nanoparticle size. Morphology, microstructure, and magnetic behavior. *Chem. Mater.*, **1999**, *11(1)*, 141-147.

[68] Kahn, H.R.; Petrikowski, K. Anisotropic structural and magnetic properties of arrays of $Fe_{26}Ni_{74}$ nanowires electrodeposited in the pores of anodic alumina. *J. Magn. Magn. Mater.*, **2000**, *215-216*, 526-528.

[69] Alexandrescu, R.; Morjan, I.; Voicu, I.; Dumitrache, F.; Albu, L.; Soare, I.; Prodan, G. Combining resonant/non-resonant processes: Nanometer-scale iron-based material preparation *via* CO_2 laser pyrolysis. *Appl. Surf. Sci.*, **2005**, *248(1-4)*, 138-146.

[70] Abu Mukh-Qasem, R.; Gedanken, A. Sonochemical synthesis of stable hydrosol of Fe_3O_4 nanoparticles. *J. Colloid Interface Sci.*, **2005**, *284(2)*, 489-494.

[71] Kim, E.H.; Lee, H.S.; Kwak, B.K.; Kim, B.-K. Synthesis of ferrofluid with magnetic nanoparticles by sonochemical method for MRI contrast agent. *J. Magn. Magn. Mater.*, **2005**, *289*, 328-330.

[72] Lefebure, S.; Dubois, E.; Cabuil, V.; Neveu, S.; Massart, R. Monodisperse magnetic nanoparticles: Preparation and dispersion in water and oils. *J. Mater. Res.*, **1998**, *13*, 2975-2981.

[73] Schwertmann, U.; Cornell, R.M. *Iron Oxides in the Laboratory: Preparation and Characterization*, VCH, Weinheim, **2000**.

[74] Palmacci, S.; Josephson, L. Synthesis of polysaccharide covered superparamagnetic oxide colloids, US Patent 5262176 **1993**.

[75] Cornell, R.M.; Schwertmann, U. *The Iron Oxides: Structure, Properties, Reactions, Occurrence and Uses*, VCH Publishers, Weinheim, **1996**.

[76] Fauconnier, N.; Bee, A.; Roger, J.; Pons, J.N. Adsorption of gluconic and citric acids on maghemite particles in aqueous medium. In: *Trends in Colloid and Interface Science X Progr. Colloid Polymer Sci.*, **1996**, *100*, 212-216.

[77] Bee, A.; Massart, R.; Neveu, S. Synthesis of very fine maghemite particles. *J. Magn. Magn. Mater.*, **1995**, *149*, 6-9.

[78] Krishnamurti G.S.R.; Huang P.M. Formation of lepidocrocite from iron (II) solutions: stabilization by citrate. *Soil Sci. Am. J.*, **1993**, 57(3), 861-867.

[79] Huang, P.M.; Wang, M.K. in « *Soils and Environment - Advances in Geoecology, Vol. 30 – Soil Processes from Mineral to Landscape Scale* » (Eds.: K. Auerswald, H. Stanjek, J. M. Bigham), International Development Centre, Ottawa, **1997**, 241-306.

[80] Liu, C.; Huang, P.M. Atomic force microscopy and surface characteristics of iron oxides formed in citrate solutions. *Soil Sci. Am. J.*, **1999**, *63(1)*, 65-72.

[81] Kodama, H.; Schnitzer, M. Effect of fulvic acid on the crystallization of Fe(III) oxides. *Geoderma*, **1977**, *19(4)*, 279-291.

[82] Kandori, K.; Kawashima, Y.; Ishikawa, T. Effects of citrate ions on the formation of monodispersed cubic hematite particles. *J. Colloid Interface Sci.*, **1992**, *152(1)*, 284-288.

[83] Kandori, K.; Kawashima, Y.; Ishikawa, T. Effects of citrate ions on the formation of ferric oxide hydroxide particles. *J. Mater. Sci.*, **1991**, *26(12)*, 3313-3319.

[84] Sahoo, Y.; Pizem, H.; Fried, T.; Golodnitsky, D.; Burstein, L.; Sukenik, C.N.; Markovich, G. Alkyl phosphonate/phosphate coating on magnetite nanoparticles: A comparison with fatty acids. *Langmuir*, **2001**, *17(25)*, 7907-7911.

[85] Lesnikovich, A.E.; Shunkevich, T.M.; Naumenko, V.N.; Vorobyova, S.A.; Baykov, M.W. Dispersity of magnetite in magnetic liquids and the interaction with a surfactant. *J. Magn. Magn. Mater.*, **1990**, *85(1-3)*, 14-16.

[86] Grants, A.; Irbitis, A.; Kronkaln, G.; Maiorov, M.M. Rheological properties of magnetite magnetic fluid. *J. Magn. Magn. Mater.*, **1990**, *85*, 129-132.

[87] Hyeon, T.; Lee, S.S.; Park, J.; Chung, Y.; Na, H.B. Synthesis of highly crystalline and monodisperse maghemite nanocrystallites without a size-selection process. *J. Am. Chem. Soc.*, **2001**, *123(51)*, 12798-12801.

[88] Khalafalla, S.E.; Reimers, G.W. Preparation of dilution-stable aqueous magnetic fluids. *IEEE Trans. Magn.*, **1980**, *16(2)*, 178-183.

[89] Shimoiizaka, J.; Nakatsuka, K.; Fujita, T.; Kounosu, A. Sink-float separators using permanent magnets and water based magnetic fluid. *IEEE Trans. Magn.*, **1980**, *16*(2), 368-371.

[90] Shen, L; Stachowiak, A.; Seif-Eddeen, K.F.; Laibinis, P.E.; Hatton, T.A. Structure of alkanoic acid stabilized magnetic fluids. A small-angle neutron and light scattering analysis. *Langmuir*, **2001**, *17(2)*, 288-299.

[91] Kondo, A.; Kamura, H.; Higashitani, K. Development and application of thermo-sensitive magnetic immunomicrospheres for antibody purification. *Appl. Microbiol. Biotechnol.*, **1994**, *41(1)*, 99-105.

[92] Shen, L.; Stachowiak, A.; Hatton, T. A.; Laibinis, P.E. Polymerization of olefin-terminated surfactant bilayers on magnetic fluid nanoparticles. *Langmuir*, **2000**, *16(25)*, 9907-9911.

[93] Hyuk Im, S.; Herricks, T.; Tack Lee, Y.; Xia, Y. Synthesis and characterization of monodisperse silica colloids loaded with superparamagnetic iron oxide nanoparticles. *Chem. Phys. Lett.*, **2005**, *40 (1-3)*, 19-23.

[94] Groman, E.V.; Josephson, L.; Lewis, J.M. Biologically degradable superparamagnetic materials for use in clinical applications. US Patent 4827945, **1989**.

[95] Pardoe, H.; Chua-anusorn, W.; St. Pierre, T.G.; Dobson, J. Structural and magnetic properties of nanoscale iron oxide particles synthesized in the presence of dextran or polyvinyl alcohol. *J. Magn. Magn. Mater.*, **2001**, *225(1-2)*, 41-46.

[96] Molday, R.S.; MacKenzie, D. Immunospecific ferromagnetic iron-dextran reagents for the labeling and magnetic separation of cells. *J. Immunol. Meth.*, **1982**, *52(3)*, 353-367.

[97] Mohapatra, S.; Pramanik, N.; Ghosh, S.K.; Pramanik, P. Synthesis and characterization of ultrafine poly(vinylalcohol phosphate) coated magnetite nanoparticles. *J. Nanosci. Nanotechnol.*, **2006**, *6(3)*, 823-829.

[98] Mendenhall, G.D.; Geng, Y.; Hwang, J. Optimization of long-term stability of magnetic fluids from magnetite and synthetic polyelectrolytes. *J. Colloid Interface Sci.*, **1996**, *184(2)*, 519-526.

[99] Wormuth, K. Superparamagnetic latex *via* inverse emulsion polymerization *J. Colloid Interface Sci.*, **2001**, *241(2)*, 366-377.

[100] Ding, X.B.; Sun, Z.H.; Wan, G.X.; Jiang, Y.Y. Preparation of thermosensitive magnetic particles by dispersion polymerization. *React. Funct. Polym.*, **1998**, *38*, 11-15.

[101] Kim, D.K.; Zhang, Y.; Kehr, J.; Klason, T.; Bjelke, B.; Muhammed, M. Characterization and MRI study of surfactant-coated superparamagnetic nanoparticles administered into the rat brain *J. Magn. Magn. Mater.*, **2001**, *225(1-2)*, 256-261.

[102] Tamaura, Y.; Takahasi, K.; Kodera, Y.; Saito, Y.; Inada, Y. Chemical modification of lipase with ferromagnetic modifier — A ferromagnetic-modified lipase. *Biotechnol. Lett.*, **1986**, *8(12)*, 877-880.

[103] Li, G.; Fan, J.; Jiang, R.; Gao, Y. Cross-linking the linear polymeric chains in the ATRP synthesis of iron oxide/polystyrene core/shell nanoparticles. *Chem. Mater.*, **2004**, *16(10)*, 1835-1837.

[104] Matyjaszewski, K.; Xia, J. Atom transfer radical polymerization. *Chem. Rev.*, **2001**, *101(9)*, 2921-2290.

[105] Sun, E.Y.; Josephson, L.; Kelly, K.A.; Weissleder, R. Development of nanoparticle libraries for biosensing. *Bioconjug. Chem.*, **2006**, *17*, 109-113.

[106] Högemann, D.; Josephson, L.; Weissleder, R.; Basilion, J.P. Improvement of MRI probes to allow efficient detection of gene expression. *Bioconjug. Chem.*, **2000**, *11*, 941-946.

[107] Josephson, L.; Tung, C.H.; Moore, A.; Weissleder, R. High-efficiency intracellular magnetic labeling with novel superparamagnetic-tat peptide conjugates. *Bioconjug. Chem.*, **1999**, *10*, 186-191.

[108] Halbreich, A.; Roger, J.; Pons, J.N.; Da Silva, A.; Hasmonay, E.; Roudier, M.; Boynard, M.; Sestier, C.; Amri, A.; Geldwerth, D.; Fertil, B.; Bacri, J.C.; Sabolovic, D. Magnetic maghemite nanoparticles : their preparation, properties, and application in cell sorting and characterization of cellular membranes *in vitro*. in: « Scientific and Clinical Applications of Magnetic Carriers », (Hafeli *et al*., Ed) Plenum Press, New-York, **1997**, *31*, 399-417.

[109] Halbreich, A.; Roger, J.; Pons, J.N.; Da Silva, A.; Bacri, J.C. Functional ferrofluids for biomedical applications, Microspheres, microcapsules & liposomes. in: « MML Series, Vol 3: Radiolabeled and Magnetic Particulates in Medicine & Biology», (R. Arshady, Ed) Citus Books, **2001**, *15*, 459-493.

[110] Cao, J.; Wang, Y.; Yu, J.; Xia, J.; Zhang, C.; Yin, D.; Hafeli, U.O. Preparation and radiolabeling of surface-modified magnetic nanoparticles with rhenium-188 for magnetic targeted radiotherapy. *J. Magn. Magn. Mater.*, **2004**, *277(1-2)*, 165-174.

[111] Whitehead, R.A.; Chagnon, M.S.; Groman, E.V.; Josephson, L. Magnetic particles for use in separations. US Patent 4,695,392, **1987**.

[112] Arkles, B. Tailoring surfaces with silanes. *Chem. Tech.*, **1977**, *7(12)*, 766-770.

[113] Brandriss, S.; Margel, S. Synthesis and characterization of self-assembled hydrophobic monolayer coatings on silica colloids. *Langmuir*, **1993**, *9(5)*, 1232-1240.

[114] Wikstrom, P.; Mandenius, C.F.; Larsson, P.O. Gas phase silylation, a rapid method for preparation of high-performance liquid chromatography supports. *J. Chromatog. A.*, **1998**, *455*, 105-117.

[115] Sun, E.Y.; Josephson, L.; Weissleder, R. "Clickable" nanoparticles for targeted imaging. *Mol. Imaging*, **2006**, *5(2)*, 122-128.

[116] Koh, I.; Wang, X.; Varughese, B.; Isaacs, L.; Ehrman S.H.; English, D.S. Magnetic iron oxide nanoparticles for biorecognition: evaluation of surface coverage and activity. *J. Phys. Chem.*, **2006**, *110*, 1553-1558.

[117] Dyal, A.; Loos, K.; Noto, M.; Chang, S.W.; Spagnoli, C.; Shafi, K.V.; Ulman, A.; Cowman, M.; Gross, R.A. Activity of Candida rugosa lipase immobilized on gamma-Fe_2O_3 magnetic nanoparticles. *J. Am. Chem. Soc.*, **2003**, *125(7)*, 1684-1685.

[118] Mikhaylova, M.; Kim, D.K.; Bobrysheva, N.; Osmolowsky, M.; Semenov, V.; Tsakalakos, T.; Muhammed, M. Superparamagnetism of magnetite nanoparticles: dependence on surface modification. *Langmuir*, **2004**, *20(6)*, 2472-2477.

[119] Takafuji, M.; Ide, S.; Ihara, H.; Xu, Z. Preparation of Poly(1-vinylimidazole)-Grafted Magnetic Nanoparticles and Their Application for Removal of Metal Ions. *Chem. Mater.*, **2004**, 16*(10)*, 1977–1983.

[120] Kaiser, R.; Miskolczy, G. Magnetic properties of stable dispersions of subdomain magnetite particles. *J. Appl. Phys.*, **1970**, *41(3)*, 1064-1072.

[121] Rao, S.; Houska, C.R. X-ray particle-size broadening. *Acta Crystallogr. A.*, **1986**, *42(1)*, 6-13.

[122] Calvin, S.; Riedel, C.; Carpenter, E.; Morrison, S.; Stroud, R.; Harris. V. Estimating crystallite size in polydispersed samples using EXAFS**.** *Phys. Cripta* T115, **2005**, 744-748.

[123] Wertheim, G.K. Mossbauer Effect: Principles and Applications. Academic Press, New York, **1964**, 239-296.

[124] De Jaeger, N.; Demeye, H.; Findy, R.; Sneyer, R.; Vanderdeelen, J.; van der Meeren, P.; Laethem, M. Particle sizing by photon correlation spectroscopy Part I: Monodisperse latices: Influence of scattering angle and concentration of dispersed material. *Part. Part. Syst. Charact.*, **1991**, *8(1-4)*, 179-203.

[125] Muller, R.N.; Roch, A.; Colet, J.M.; Ouakssim, A.; Gillis, P. Particulate magnetic contrast agents. in: « The Chemistry of Contrast Agents in Medical Magnetic Resonance Imaging », (A.E. Merbach and E. Toth, Eds) Wiley, **2001**, *10*, 417-435.

[126] Roch, A.; Gillis, P.; Ouakssim, A.; Muller, R.N. Proton magnetic relaxation in superparamagnetic aqueous colloids: a new tool for the investigation of ferrite crystal anisotropy. *J. Magn. Magn. Mater*., **1999**, *201*, 77-79.

[127] Ouakssim, A.; Fastrez, S.; Roch, A.; Laurent, S.; Gossuin, Y.; Pierart, C.; Vander Elst, L.; Muller, R.N. Control of the synthesis of magnetic fluids by relaxometry and magnetometry. *J. Magn. Magn. Mater*., **2004**, *72*, E1711-E1713.

[128] Solomon, I. Relaxation processes in a system of two spins. *Phys. Rev.*, **1955**, *99(2)*, 559-565.

[129] Bloembergen, N.J. Proton relaxation times in paramagnetic solutions. *J. Chem. Phys.*, **1957**, *27(2)*, 572-573.

[130] Freed, J.H. Dynamic effects of pair correlation functions on spin relaxation by translational diffusion in liquids. II. Finite jumps and independent T_1 processes. *J. Chem. Phys.*, **1978**, *68(9)*, 4034-4037.

[131] Wang, Y.X.; Hussain, S.M.; Krestin, G.P. Superparamagnetic iron oxide contrast agents: physicochemical characteristics and applications in MR imaging. *Eur. Radiol.*, **2001**, *11*, 2319-2331.

[132] Shen, T.; Weissleder, R.; Papisov, M.; Bogdanov, A.; Brady, T.J. Monocrystalline iron oxide nanocompounds (MION): physicochemical properties. *Magn. Reson. Med.*, **1993**, *29*, 599-604.

[133] Arbab, A.S.; Liu, W.; Frank, J.A. Cellular magnetic resonance imaging: current status and future prospects. *Expert Rev. Med. Devices*, 2006, *3*, 427-439.

[134] Taupitz, M.; Wagner, S.; Schnorr, J.; Kravec, I.; Pilgrimm, H.; Bergmann-Fritsch, H.; Hamm, B. Phase I clinical evaluation of citrate-coated monocrystalline very small superparamagnetic iron oxide particles as a new contrast medium for magnetic resonance imaging. *Invest. Radiol.*, **2004**, *39*, 394-405.

[135] Weissleder, R.; Stark, D.D.; Engelstad, B.L.; Bacon, B.R.; Compton, C.C.; White, D.L.; Jacobs, P.; Lewis, J. Superparamagnetic iron oxide: pharmacokinetics and toxicity. *Am. J. Roentgenol.*, **1989**, *152*, 167-173.

[136] Vasseur, S.; Grasset, F.; Duguet, E. Magnetic nanoparticle design for medical diagnosis and therapy. *J. Mater. Chem.*, **2004**, *14*, 2161-2175.

[137] Weinmann, H.J.; Ebert, W.; Misselwitz, B.; Schmitt-Willich, H. Tissue-specific MR contrast agents. *Eur. J. Radiol.*, **2003**, *46*, 33-44.

[138] Jain, T.K.; Reddy, M.K.; Morales, M.A.; Leslie-Pelecky, D.L.; Labhasetwar, V. Biodistribution, clearance, and biocompatibility of iron oxide magnetic nanoparticles in rats. *Mol. Pharm.*, **2008**, *5(2)*, 316-327.

[139] Bourrinet, P.; Bengele, H.H; Bonnemain, B.; Dencausse, A.; Idee, J.M.; Jacobs, P.M.; Lewis, J.M. Preclinical safety and pharmacokinetic profile of ferumoxtran-10, an ultrasmall superparamagnetic iron oxide magnetic resonance contrast agent. *Invest. Radiol.*, **2006**, *41(3)*, 313-324.

[140] Wagner, S.; Schnorr, J.; Pilgrimm, H.; Hamm, B.; Taupitz, M. Monomer-coated very small superparamagnetic iron oxide particles as contrast medium for magnetic resonance imaging: preclinical *in vivo* characterization. *Invest. Radiol.*, **2002**, *37(4)*, 167-177.

[141] Oksendal, A.N.; Hals, P.A. Biodistribution and toxicity of MR imaging contrast media. *J. Magn. Reson. Imaging*, **1993**, *3(1)*, 157-165.

[142] Bulte, J.W.; Kraitchman, D.L. Iron oxide MR contrast agents for molecular and cellular imaging. *NMR Biomed.*, **2004**, *17*, 484-499.

[143] Sykova, E.; Jendelova, P. Magnetic resonance tracking of implanted adult and embryonic stem cells in injured brain and spinal cord. *Ann. N. Y. Acad. Sci.*, **2005**, *1049*, 146-160.

[144] Tallheden, T.; Nanmark, U.; Lorentzon, M.; Rakotonirainy, O.; Soussi, B.; Waagstein, F.; Jeppsson, A.; Sjogren-Jansson, E.; Lindhal, A.; Omerovic, E. *In vivo* MR imaging of magnetically labeled human embryonic stem cells. *Life Sci.*, **2006**, *79*, 999-1006.

[145] Amsalem, Y.; Mardor, Y.; Feinberg, M.S.; Landa, N.; Miller, L.; Daniels, D.; Ocherashvilli, A.; Holbova, R.; Yosef, O.; Barbash, I.M.; Leor, J. Iron-oxide labeling and outcome of transplanted mesenchymal stem cells in the infarcted myocardium. *Circulation*, **2007**, *116*, 138-145.

[146] Ittrich, H.; Lange, C.; Tögel, F.; Zander, A.R.; Dahnke, H.; Westenfelder, C.; Adam, G.; Nolte-Ernsting, C. *In vivo* magnetic resonance imaging of iron oxide-labeled, arterially-injected mesenchymal stem cells in kidneys of rats with acute ischemic kidney injury: detection and monitoring at 3T. *J. Magn. Reson. Imaging*, **2007**, *25*, 1179-1191.

[147] Ju, S.; Teng, G.J.; Lu, H.; Zhang, Y.; Zhang, A.; Chen, F.; Ni, Y. *In vivo* MR tracking of mesenchymal stem cells in rat liver after intrasplenic transplantation. *Radiology*, **2007**, *245*, 206-215.

[148] Smirnov, P.; Lavergne, E.; Gazeau, F.; Lewin, M.; Boissonnas, A.; Doan, B.T.; Gillet, B.; Combadière, C.; Combadière, B.; Clément, O. *In vivo* cellular imaging of lymphocyte trafficking by MRI: a tumor model approach to cell-based anticancer therapy. *Magn. Reson. Med.*, **2006**, *56*, 498-508.

[149] Arbab, A.S.; Rad, A.M.; Iskander, A.S.; Jafari-Khouzani, K.; Brown, S.L.; Churchman, J.L.; Ding, G.; Jiang, Q.; Frank, J.A.; Soltanian-Zadeh, H.; Peck, D.J. Magnetically-labeled sensitized splenocytes to identify glioma by MRI: a preliminary study. *Magn. Reson. Med.*, **2007**, *58*, 519-526.

[150] Wu, X.; Hu, J.; Zhou, L.; Mao, Y.; Yang, B.; Gao, L.; Xie, R.; Xu, F.; Zhang, D.; Liu, J.; Zhu, J. *J. Neurosurg.*, **2008**, *108*, 320-329.

[151] Valable, S.; Barbier, E.L.; Bernaudin, M.; Roussel, S.; Segebarth, C.; Petit, E.; Rémy, C. *In vivo* MRI tracking of exogenous monocytes/macrophages targeting brain tumors in a rat model of glioma. *Neuroimage*, **2008**, *40*, 973-983.

[152] Berry, C.C.; Wells, S.; Charles, S.; Aitchison, G.; Curtis, A.S. Cell response to dextran-derivatised iron oxide nanoparticles post internalisation. *Biomaterials*, **2004**, *25*, 5405-5413.

[153] Hsiao, J.K.; Tai, M.F.; Chu, H.H.; Chen, S.T.; Li, H.; Lai, D.M.; Hsieh, S.T.; Wang, J.L.; Liu, H.M. Magnetic nanoparticle labeling of mesenchymal stem cells without transfection agent: cellular behavior and capability of detection with clinical 1.5 T magnetic resonance at the single cell level. *Magn. Reson. Med.*, **2007**, *58*, 717-724.

[154] Raynal, I.; Prigent, P.; Peyramaure, S.; Najid, A.; Rebuzzi, C.; Corot, C. Macrophage endocytosis of superparamagnetic iron oxide nanoparticles: mechanisms and comparison of ferumoxides and ferumoxtran-10. *Invest. Radiol.*, **2004**, *39*, 56-63.

[155] Matuszewski, L.; Persigehl, T.; Wall, A.; Schwindt, W.; Tombach, B.; Fobker, M.; Poremba, C.; Ebert, W.; Heindel, W.; Bremer, C. Cell tagging with clinically approved iron oxides: feasibility and effect of lipofection, particle size, and surface coating on labeling efficiency. *Radiology*, **2005**, *235*, 155-161.

[156] Tung, C.H.; Weissleder, R. Arginine containing peptides as delivery vectors. *Adv. Drug Deliv. Rev.*, **2003**, *55*, 281-294.

[157] Song, M.; Moon, W.K.; Kim, Y.; Lim, D.; Song , I.C.; Yoon, B.W. Labeling efficacy of superparamagnetic iron oxide nanoparticles to human neural stem cells: comparison of ferumoxides, monocrystalline iron oxide, cross-linked iron oxide (CLIO)-NH_2 and tat-CLIO. *Korean J. Radiol.*, **2007**, *8*, 365-371. Erratum in *Korean J. Radiol.*, **2008**, *9*, 94.

[158] Mailänder, V.; Lorenz, M.R.; Holzapfel, V.; Musyanovych, A.; Fuchs, K.; Wiesneth, M.; Walther, P.; Landfester, K.; Schrezenmeier, H. Carboxylated superparamagnetic iron oxide particles label cells intracellularly without transfection agents. *Mol. Imaging Biol.*, **2008**, *10*, 138-146.

[159] Boutry, S.; Brunin, S.; Mahieu, I.; Laurent, S.; Vander Elst, L.; Muller, R.N. Magnetic labeling of non-phagocytic adherent cells with iron oxide nanoparticles: a comprehensive study. *Contrast Med. Mol. Imaging.*, **2008**, *3(6)*, 223-232.

[160] Metz, S.; Bonaterra, G.; Rudelius, M.; Settles, M.; Rummeny, E.J.; Daldrup-Link, H.E. Capacity of human monocytes to phagocytose approved iron oxide MR contrast agents *in vitro*. *Eur. Radiol.*, **2004**, *14*, 1851-1858.

[161] Jirak, D.; Kriz, J.; Herynek, V.; Andersson, B.; Girman, P.; Burian, M.; Saudek, F.; Hajek, M. MRI of transplanted pancreatic islets. *Magn. Reson. Med.*, **2004**, *52*, 1228-1233.

[162] Evgenov, N.V.; Medarova, Z.; Pratt, J.; Pantazopoulos, P.; Leyting, S.; Bonner-Weir, S.; Moore, A. *In vivo* imaging of immune rejection in transplanted pancreatic islets. *Diabetes*, **2006**, *55*, 2419-2428.

[163] Shapiro, E.M.; Sharer, K.; Skrtic, S.; Koretsky, A.P. *In vivo* detection of single cells by MRI. *Magn. Reson. Med.*, **2006**, *55*, 242-249.

[164] Arbab, A.S.; Bashaw, L.A.; Miller, B.R.; Jordan, E.K.; Bulte, J.W.; Frank, J.A. Intracytoplasmic tagging of cells with ferumoxides and transfection agent for cellular magnetic resonance imaging after cell transplantation: methods and techniques. *Transplantation*, **2003**, *76*, 1123-1130.

[165] van den Bos, E.J.; Wagner, A.; Mahrholdt, H.; Thompson, R.B.; Morimoto, Y.; Sutton, B.S.; Judd, R.M.; Taylor, D.A. Improved efficacy of stem cell labeling for magnetic resonance imaging studies by the use of cationic liposomes. *Cell Transplant.*, **2003**, *12*, 743-756.

[166] Pawelczyk, E.; Arbab, A.S.; Pandit, S.; Hu, E.; Frank, J.A. Expression of transferrin receptor and ferritin following ferumoxides-protamine sulfate labeling of cells: implications for cellular magnetic resonance imaging. *NMR Biomed.*, **2006**, *19*, 581-592.

[167] Dousset, V.; Doche, B.; Petry, K.G.; Brochet, B.; Delalande, C.; Caille, J.M. Correlation between clinical status and macrophage activity imaging in the central nervous system of rats. *Acad. Radiol.*, **2002**, *9 Suppl 1*, S156-S159.

[168] Jander, S.; Schroeter, M.; Saleh, A. Imaging inflammation in acute brain ischemia. *Stroke*, **2007**, *38*, 642-645.

[169] Corot, C.; Petry, K.G.; Trivedi, R.; Saleh, A.; Jonkmanns, C.; Le Bas, J.F.; Blezer, E.; Rausch, M.; Brochet, B.; Foster-Gareau, P.; Balériaux, D.; Gaillard, S.; Dousset, V. Macrophage imaging in central nervous system and in carotid atherosclerotic plaque using ultrasmall superparamagnetic iron oxide in magnetic resonance imaging. *Invest. Radiol.*, **2004**, *39*, 619-625.

[170] Simon, G.H.; von Vopelius-Feldt, J.; Fu, Y.; Schlegel, J.; Piontek, G; Wendland, M.F.; Chen, M.H.; Daldrup-Link, H.E. Ultrasmall superparamagnetic iron oxide-enhanced magnetic resonance imaging of antigen-induced arthritis: a comparative study between SHU 555 C, ferumoxtran-10, and ferumoxytol. *Invest. Radiol.*, **2006**, *41*, 45-51.

[171] Petry, K.G.; Boiziau, C.; Dousset, V.; Brochet, B. Magnetic resonance imaging of human brain macrophage infiltration. *Neurotherapeutics*, **2007**, *4*, 434-442.

[172] Zimmer, C.; Wright Jr, S.C.; Engelhardt, R.T.; Johnson, G.A.; Kramm, C.; Breakefield, X.O.; Weissleder, R. Tumor cell endocytosis imaging facilitates delineation of the glioma-brain interface. *Exp. Neurol.*, **1997**, *143*, 61-69.

[173] Muldoon, L.L.; Sandor, M.; Pinkston, K.E.; Neuwelt, E.A. Imaging, distribution, and toxicity of superparamagnetic iron oxide magnetic resonance nanoparticles in the rat brain and intracerebral tumor. *Neurosurgery*, **2005**, *57*, 785-796.

[174] Beckmann, N.; Cannet, C.; Fringeli-Tanner, M.; Baumann, D.; Pally, C.; Bruns, C.; Zerwes, H.G.; Andriambeloson, E.; Bigaud, M. Macrophage labeling by SPIO as an early marker of allograft chronic rejection in a rat model of kidney transplantation. *Magn. Reson. Med.*, **2003**, *49*, 459-467.

[175] Kleinschnitz, C.; Bendszus, M.; Frank, M.; Solymosi, L.; Toyka, K.V.; Stoll, G. *In vivo* monitoring of macrophage infiltration in experimental ischemic brain lesions by magnetic resonance imaging. *J. Cereb. Blood Flow Metab.*, **2003**, *23*, 1356-1361.

[176] Wu, Y.L.; Ye, Q.; Foley, L.M.; Hitchens, T.K.; Sato, K.; Williams, J.B.; Ho, C. In situ labeling of immune cells with iron oxide particles: an approach to detect organ rejection by cellular MRI. *Proc. Natl. Acad. Sci. U S A.*, **2006**, *103*, 1852–1857.

[177] von Zur Muhlen, C.; von Elverfeldt, D.; Bassler, N.; Neudorfer, I.; Steitz, B.; Petri-Fink, A.; Hofmann, H.; Bode, C.; Peter, K. Superparamagnetic iron oxide binding and uptake as imaged by magnetic resonance is mediated by the integrin receptor Mac-1 (CD11b/CD18): implications on imaging of atherosclerotic plaques. *Atherosclerosis,* **2007**, *193*, 102-111.

[178] Brillet, P.Y.; Gazeau, F.; Luciani, A.; Bessoud, B.; Cuenod, C.A.; Siauve, N.; Pons, J.N.; Poupon, J.; Clément, O. Evaluation of tumoral enhancement by superparamagnetic iron oxide particles: comparative studies with ferumoxtran and anionic iron oxide nanoparticles. *Eur. Radiol.*, **2005**, *15*, 1369-1377.

[179] Shapiro, E.M.; Gonzalez-Perez, O.; Garcia-Verdugo, J.M.; Alvarez-Buylla, A.; Koretsky, A.P. Magnetic resonance imaging of the migration of neuronal precursors generated in the adult rodent brain. *Neuroimage*, **2006**, *32*, 1150-1157.

[180] Petropoulos, A.E.; Schaffer, B.K.; Cheney, M.L.; Enochs, S.; Zimmer, C.; Weissleder, R. MR imaging of neuronal transport in the guinea pig facial nerve: initial findings. *Acta Otolaryngol.*, **1995**, *115*, 512-516.

[181] van Everdingen, K.J.; Enochs, W.S.; Bhide, P.G.; Nossiff, N.; Papisov, M.; Bogdanov Jr, A.; Brady, T.J.; Weissleder, R. Determinants of *in vivo* MR imaging of slow axonal transport. *Radiology,* **1994**, *193*, 485-491.

[182] Neuwelt, E.A.; Weissleder, R.; Nilaver, G.; Roman-Goldstein, S.; Szumowski, J.; Pagel, M.A.; Kroll, R.A.; Remsen, L.G.; McCormick, C.I.; Jones, R.S.; Shannon, E.M.; Muldoon, L.L. Delivery of virus-sized iron oxide particles to rodent CNS neurons. *Neurosurgery*, **1994**, *34*, 777-784.

[183] Högemann-Savellano, D.; Bos, E.; Blondet, C.; Sato, F.; Abe, T.; Josephson, L.; Weissleder, R.; Gaudet, J.; Sgroi, D.; Peters, P.J.; Basilion, J.P. The transferrin receptor: a potential molecular imaging marker for human cancer. *Neoplasia*, **2003**, *5*, 495-506.

[184] Sonvico, F.; Vasseur, S.; Dubernet, C.; Jaillard, D.; Degrouard, J.; Hoebeke, J.; Duguet, E.; Colombo, P.; Couvreur, P. Folate-conjugated iron oxide nanoparticles for solid tumor targeting as potential specific magnetic hyperthermia mediators: synthesis, physicochemical characterization, and *in vitro* experiments. *Bioconjug. Chem.*, **2005**, *16*, 1181-1188.

[185] Pirko, I.; Johnson, A.; Ciric, B.; Gamez, J.; Macura, S.I.; Pease, L.R.; Rodriguez, M. *In vivo* magnetic resonance imaging of immune cells in the central nervous system with superparamagnetic antibodies. *FASEB J.*, **2004**, *18*, 179-182.

[186] Medarova, Z.; Tsai, S.; Evgenov, N.; Santamaria, P.; Moore, A. *In vivo* imaging of a diabetogenic CD8+ T cell response during type 1 diabetes progression. *Magn. Reson. Med.*, **2008**, *59*, 712-720.

[187] Zhang, C.; Jugold, M.; Woenne, E.C.; Lammers, T.; Morgenstern, B.; Mueller, M.M.; Zentgraf, H.; Bock, M.; Eisenhut, M.; Semmler, W.; Kiessling, F. Specific targeting of tumor angiogenesis by RGD-conjugated ultrasmall superparamagnetic iron oxide particles using a clinical 1.5-T magnetic resonance scanner. *Cancer Res.*, **2007**, *67*, 1555-1562.

[188] Montet, X.; Montet-Abou, K.; Reynolds, F.; Weissleder, R.; Josephson, L. Nanoparticle imaging of integrins on tumor cells. *Neoplasia,* **2006**, *8*, 214-222.

[189] Sun, C.; Veiseh, O.; Gunn, J.; Fang, C.; Hansen, S.; Lee, D.; Sze, R.; Ellenbogen, R.G.; Olson, J.; Zhang, M. *In vivo* MRI detection of gliomas by chlorotoxin-conjugated superparamagnetic nanoprobes. *Small,* **2008**, *4*, 372-379.

[190] Oyewumi, M.O.; Yokel, R.A.; Jay, M.; Mumper, R.J. Comparison of cell uptake, biodistribution and tumor retention of folate-coated and PEG-coated gadolinium nanoparticles in tumor-bearing mice. *J. Control Release,* **2004**, *95*, 613-626.

[191] Leuschner, C.; Kumar, C.S.; Hansel, W.; Soboyejo, W.; Zhou, J.; Hormes, J. LHRH-conjugated magnetic iron oxide nanoparticles for detection of breast cancer metastases. *Breast Cancer Res. Treat.*, **2006**, *99*, 163-176.

[192] Serda, R.E.; Adolphi, N.L.; Bisoffi, M.; Sillerud, L.O. Targeting and cellular trafficking of magnetic nanoparticles for prostate cancer imaging. *Mol. Imaging,* **2007**, *6*, 277-288.

[193] Smith, B.R.; Heverhagen, J.; Knopp, M.; Schmalbrock, P.; Shapiro, J.; Shiomi, M.; Moldovan, N.I.; Ferrari, M.; Lee, S.C. Localization to atherosclerotic plaque and biodistribution of biochemically derivatized superparamagnetic iron oxide nanoparticles (SPIONs) contrast particles for magnetic resonance imaging (MRI). *Biomed. Microdev.*, **2007**, *9*, 719-727. Erratum in *Biomed. Microdevices*, **2008**, *10*, 129-130.

[194] Kang, H.W.; Torres, D.; Wald, L.; Weissleder, R.; Bogdanov Jr, A.A. Targeted imaging of human endothelial-specific marker in a model of adoptive cell transfer. *Lab. Invest.*, **2006**, *86*, 599-609.

[195] Shapiro, E.M.; Medford-Davis, L.N.; Fahmy, T.M.; Dunbar, C.E.; Koretsky, A.P. Antibody-mediated cell labeling of peripheral T cells with micron-sized iron oxide particles (MPIOs) allows single cell detection by MRI. *Contrast Media Mol. Imaging,* **2007**, *2*, 147-153.

[196] Schellenberger, E.; Schnorr, J.; Reutelingsperger, C.; Ungethüm, L.; Meyer, W.; Taupitz, M.; Hamm, B. Linking proteins with anionic nanoparticles *via* protamine: ultrasmall protein-coupled probes for magnetic resonance imaging of apoptosis. *Small,* **2008**, *4*, 225-230.

[197] McAteer, M.A.; Sibson, N.R.; von Zur Muhlen, C.; Schneider, J.E.; Lowe, A.S.; Warrick, N.; Channon, K.M.; Anthony, D.C.; Choudhury, R.P. *In vivo* magnetic resonance imaging of acute brain inflammation using microparticles of iron oxide. *Nat. Med.*, **2007**, *13*, 1253-1258.

[198] McAteer, M.A.; Schneider, J.E.; Ali, Z.A.; Warrick, N.; Bursill, C.A.; von zur Muhlen, C.; Greaves, D.R.; Neubauer, S.; Channon, K.M.; Choudhury, R.P. Magnetic resonance imaging of endothelial adhesion molecules in mouse atherosclerosis using dual-targeted microparticles of iron oxide. *Arterioscler. Thromb. Vasc. Biol*., **2008**, *28*, 77-83.

Received: July 25, 2009 Revised: November 23, 2009 Accepted: November 25, 2009